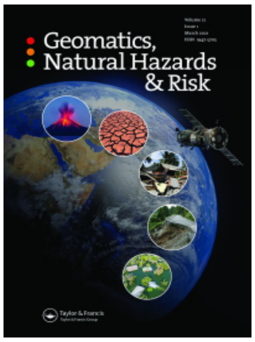

Geomatics, Natural Hazards and Risk

ISSN: (Print) (Online) Journal homepage: www.tandfonline.com/journals/tgnh20

Assessing climate trends in the Northwestern Himalayas: a comprehensive analysis of high-resolution gridded and observed datasets

Rayees Ahmed, Taha Shamim, Joshal Kumar Bansal, Abid Farooq Rather, Sumaira Javaid, Gowhar Farooq Wani, Ishfaq Hussain Malik, Pervez Ahmed, Sanjay K. Jain, Kashif Imdad, James D. Ford & Riyaz A. Mir

GEOMATICS, NATURAL HAZARDS AND RISK
2024, VOL. 15, NO. 1, 2401994
https://doi.org/10.1080/19475705.2024.2401994

Taylor & Francis
Taylor & Francis Group

OPEN ACCESS Check for updates

Assessing climate trends in the Northwestern Himalayas: a comprehensive analysis of high-resolution gridded and observed datasets

Rayees Ahmed[a], Taha Shamim[a], Joshal Kumar Bansal[b], Abid Farooq Rather[a], Sumaira Javaid[a], Gowhar Farooq Wani[a], Ishfaq Hussain Malik[c], Pervez Ahmed[a], Sanjay K. Jain[d], Kashif Imdad[e], James D. Ford[c,f] and Riyaz A. Mir[d]

[a]Department of Geography and Disaster Management, School of Earth and Environmental Sciences, University of Kashmir, Srinagar, India; [b]Center of Excellence in Disaster Mitigation and Management, Indian Institute of Technology, Indian Institute of Technology, Roorkee, India; [c]School of Geography, University of Leeds, Leeds, United Kingdom; [d]National Institute of Hydrology, Western Himalayan Regional Centre, Jammu and Kashmir, Jammu, India; [e]Department of Geography, Pandit Prithi Nath PG College (affiliated to Chhatrapati Shahu Ji Maharaj University), Kanpur, Uttar Pradesh, India; [f]Priestley Centre for Climate Futures, University of Leeds, Leeds, United Kingdom

ABSTRACT

Climate change poses significant challenges to the Himalayas, a region characterised by its fragile ecosystems and vulnerable communities dependent on environmental resources. Accurate climate data are crucial for understanding regional climatic variations and assessing climate change impacts, particularly in areas with limited observational networks. This study represents a pioneering effort in evaluating climatic fluctuations in the Jhelum basin, located in the North Western Himalayas, by utilising a diverse range of gridded meteorological datasets (APHRODITE, CHIRPS, CRU, and IMDAA) alongside observed climate data from the Indian Meteorological Department. The primary goal is to identify the most effective gridded climate data product for regions with limited data and to explore the potential of combining gridded data sets with observed data to understand climatic variability. Findings indicate a consistent upward trend in temperature across all datasets, with varying rates of increase. CRU records a rise of 1 °C in T*max* and 1.6 °C in T*min*, while APHRODITE shows a T*mean* increase of approximately 1 °C. IMDAA reports increases in T*max* and T*min*. Observed mean annual T*max* and T*min* show net increases of 1 °C and 0.6 °C, respectively. Regarding precipitation, all datasets except IMDAA exhibit an increasing trend, contrary to observed data, which decreases from 1266 mm to 1068 mm over 40 years. CHIRPS, CRU, and APHRODITE display increasing trends, while IMDAA aligns closely with observed data but tends to overestimate precipitation by about 30%. Our research identifies IMDAA as the most

ARTICLE HISTORY
Received 18 July 2024
Accepted 4 September 2024

KEYWORDS
Climate change; Jhelum basin, NW Himalayas; gridded data; observed data; comparative analysis

CONTACT Ishfaq Hussain Malik i.h.malik@leeds.ac.uk School of Geography, University of Leeds, Leeds, LS2 9JT, United Kingdom.

Supplemental data for this article can be accessed online at https://doi.org/10.1080/19475705.2024.2401994.

suitable gridded climate data for the Jhelum basin in the North-western Himalayas. Despite some discrepancies in precipitation trends, IMDAA closely aligns with observed data, providing valuable insights for scholars and policymakers navigating climate data uncertainties in complex environments. Our findings contribute to informed decision-making and effective climate change mitigation strategies in the region.

1. Introduction

Climate change is a critical social and environmental issue, whose effects are increasing and may become irreversible, impacting terrestrial, freshwater, cryosphere, coastal, and open ocean ecosystems (IPCC, 2023). The Himalayas have garnered significant research attention due to their role in dictating the hydro-meteorological conditions of the area, their susceptibility to climate impacts and increasing disasters, and their status as a global biodiversity hotspot (Shrestha 2009; Xu et al. 2009; Bhutiyani et al. 2010; Sabin et al. 2020; Malik and Hashmi 2022; Patel et al. 2022; Malik 2022a, 2022b; Malik and Hashmi 2021; Swain et al. 2022d; Rawat et al. 2023; Ahmed et al., 2022; Imdad et al. 2023; Malik and Ford 2024a; Rather et al. 2024). Addressing and adapting to the effects of climate change necessitates understanding of several interlinked factors (Malik and Ford 2024b) and accurate measurements of various climatic factors. Current research is delving into trend analyses (Wang et al. 2022; Swain et al. 2022a, 2022b) and future climate projections (Sharmila et al. 2015; Imbach et al. 2018; Haile et al. 2020). For any time series climate data analysis and modelling, the availability of ample and reliable data is crucial. Gridded datasets, which are often preferred due to the limited spatial and temporal coverage of observed datasets, play a pivotal role in this context (Gulizia and Camilloni 2016; Hosseini-Moghari et al. 2018; Caloiero et al. 2021). The foremost advantage of gridded datasets is their ability to encompass extensive territories and extended periods, which renders them ideal for climatic trend analysis, especially in data-scarce regions.

Several studies have utilized trend analysis of key climate variables like temperature and precipitation to understand climate change in the Himalayas (Swain et al. 2022c; Ahmad et al., 2022). Bhutiyani et al. (2007) observed a warming trend of 0.16 °C per decade in the Northwest Himalayan region during the twentieth century. Shrestha et al. (1999) documented warming trends between 0.06 °C and 0.12 °C in the Nepal Himalayas, derived from maximum temperature records collected from 49 stations in Nepal. Accelerated warming in the Himalayas was reported by Sabin et al. (2020) at a rate of 0.2 °C per decade from 1951 to 2014 in areas with elevations lower than 4000 m and a much higher rate of 0.5 °C above 4000 m. Several studies indicate that the warming trends in winter temperature were more pronounced in the Himalayas (-1.41 °C) in comparison to the global average of 0.85 °C from 1880-2012 (Shrestha et al. 1999; Singh et al. 2010; Das et al. 2018). The elevated zones of the Western Himalayas show greater sensitivity to winter temperatures due to the extensive areas of snow cover and the influence of black carbon and aerosol particles (Das et al. 2020; Ahmed et al. 2022a).

In the Jhelum basin, studies including that of Shafiq et al. (2019) have analysed temperature and precipitation patterns in the Kashmir Valley within the North-Western Himalayas across various topographical areas from 1980 to 2014. Their findings indicate a significant uptick in annual temperatures and mean annual maximum temperatures at a rate of 0.03 °C per annum, with winter temperatures rising even more sharply. In a similar vein, Lone et al. (2022) examined temperature and precipitation from 1980 to 2020 in the Kashmir Valley, observing a mean annual temperature increase of 1.55 °C, including substantial rises of 2.00 °C in mean maximum temperatures and 1.10 °C in mean minimum temperatures. However, their study also noted an insignificant downward trend in precipitation. Dash et al. (2007) identified a warming trend of 0.9 °C throughout the past century (1901–2003) in the Western Himalayas. Dad et al. (2021) documented an increase of 0.35 °C in mean maximum temperatures and 0.22 °C in mean minimum temperatures between 1980 and 2017, alongside a slight annual rise in precipitation by 0.4 mm.

Most of these previous studies like Shafiq et al. (2019) and Lone et al. (2022) demonstrate a steady rise in temperatures along with a trend towards reduced precipitation based on observed data sets. Comparative research has been conducted on various climate datasets around the globe. Andermann et al. (2011) evaluated the efficacy of different gridded climatic datasets in the area adjacent to the Himalayas. Palazzi et al. (2013) assessed the accuracy of multiple gridded datasets and found that they reliably captured the year-to-year changes in precipitation in the Hindukush Himalayas. However, ERA-interim estimations for the Karakoram were found to be consistent with the observations (Palazzi et al. 2013; Immerzeel et al. 2015; Dahri et al. 2016). In comparing the performance of TMPA 3B42V7 with APHRO 1101, Hussain et al. (2017) discovered that TMPA had a low correlation with in-situ observations. They also noticed that elevation had a significant effect on the performance of gridded datasets.

This study addresses a significant gap in existing literature by integrating observed and gridded climate data to analyse trends in climatic variables within the Jhelum basin of the Northwestern Himalayas. Previous studies conducted in this geographical area heavily relied on observed data from various stations such as Shalimar (Srinagar), Kupwara, Pahalgam, Kokernag, Gulmarg, and Qazigund to assess changes in temperature and precipitation. In contrast, this study utilises a diverse range of satellite-based temperature and precipitation products, enabling a more comprehensive and thorough evaluation. By comparing different gridded datasets, including Indian Monsoon Data Assimilation and Analysis (IMDAA), Climate Research Unit (CRU), Climate Hazards Group InfraRed Precipitation with Station (CHIRPS), and Asian Precipitation - Highly-Resolved Observational Data Integration Towards Evaluation (APHRODITE), with observed data obtained from six distinct stations within the Jhelum basin, this research introduces a new dimension to the analysis. This comparative approach is instrumental in determining the most effective dataset for the region with limited data availability. Consequently, the findings of this study yield valuable insights for future climate research in the Himalayas. The work reported in this article stands out as one of the first to utilise a comprehensive range of satellite-based temperature and precipitation products to examine the variability of climate in the Jhelum basin. Furthermore, we focused on comparative analysis of these data sets and subsequently verified their accuracy by comparing them with station data. This process is necessary to determine the level of bias present in the different gridded data sets produced by various organisations in the study area.

2. Description of the study area

The Jhelum basin, often referred as the valley of Kashmir, is situated between latitudes 32° 20′ and 34° 50′N and longitudes 73° 55′ and 75° 35′ E and is enclosed by the Great Himalayan Mountain range in the northeast and the Pir Panjal range of the lesser Himalaya in the southwest (Figure 1). The Jhelum basin spans 15,948 square kilometers and features the Jhelum River, a tributary of the Indus River, flowing through it southeast to northwest. This region typically has an average annual temperature and precipitation of 13.5 °C and 710 mm (about 2.33 ft) respectively. Most of this precipitation (∼72%) is received in the winter months from the western disturbances originating in the Mediterranean region, while a small portion (∼28%) is from the Indian Summer Monsoon (ISM).

Rainfall averages vary across the region, from around 650 mm in Srinagar to more than 1500 mm in the higher elevations of Pahalgam and Sonamarg hill stations (Ahmed et al., 2022b). Mean monthly temperatures (T_{max} and T_{min}) and precipitation of the study area from 1980 to 2020 are illustrated in Figure 1b. Glacial and snowmelt significantly influence the water flow patterns of the Jhelum basin, with the rivers reaching their maximum discharge in May and June as a result of the accelerated melting of snow and ice at higher altitudes.

The data shows that observed discharge at three stations, namely Asham, Sangam, and Ram-Munshi Bagh, is indicating a decreasing trend, as depicted in Figure 1c. The observed streamflow shows a significant drop, which is attributed to the significant loss of glacier resources in the valley (Malik et al., 2024). According to Marazi (2019), the combined contributions of snow and glacier melt account for approximately 65% of the yearly flow in the Jhelum basin. It is worth noting that the streamflow data shows a significant increase in streamflow during the years 2006, 2010, 2014 (flood year), and 2018, while it exhibits a consistent reduction from 2018 onwards. This observed trend aligns with studies indicating that greater glacier melting initially leads to higher streamflow in glacier-fed streams, followed by a subsequent decline due to diminishing ice mass.

3. Materials and methodology

3.1. Data sources

Analysis of the gridded climate datasets plays a key role in understanding climate variability over a region, especially in areas lacking meteorological observatories. They offer extensive data and insights on a range of climate-related variables over an extended period, making them ideal for use at any geographical scale (Sidau et al., 2021). These datasets have been widely utilized in previous studies to analyze trends in climate variables (Singh and Xiaosheng 2019; Caloiero et al. 2021; Reda et al. 2021;

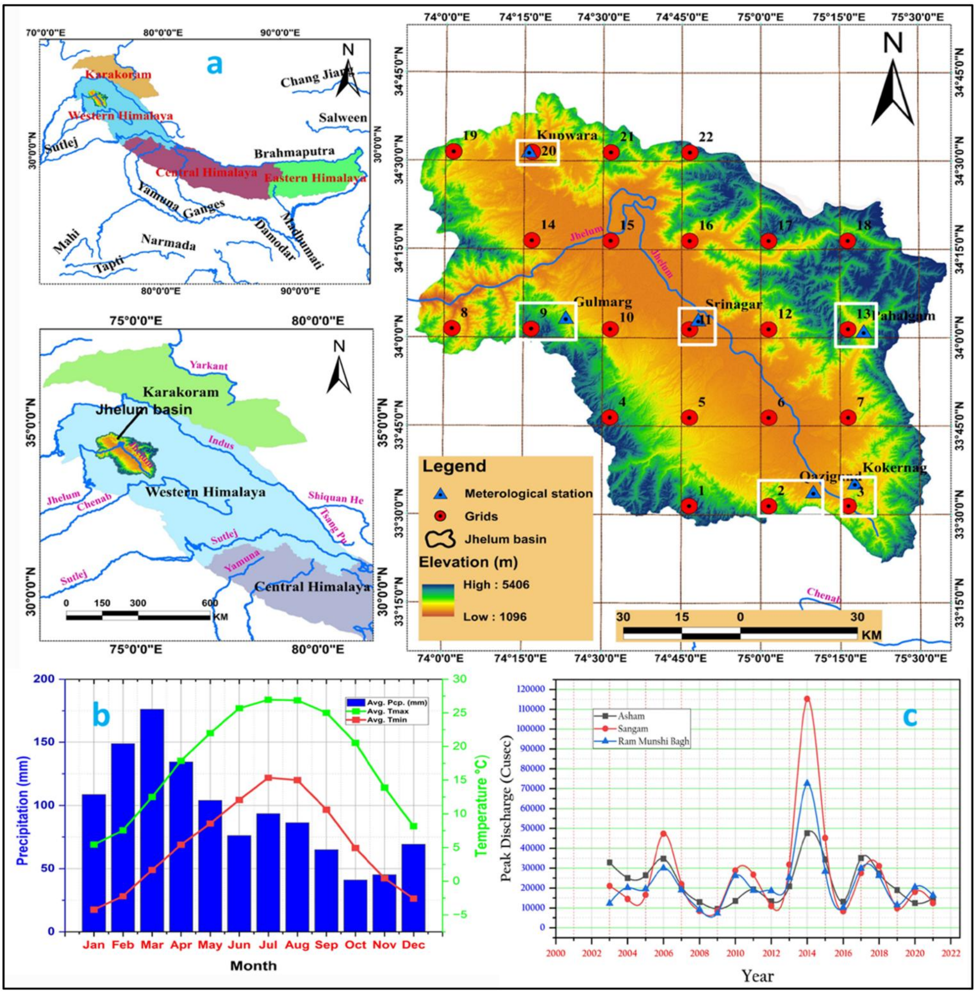

Figure 1. **a)** The study area map shows the 22 grids (red-coloured circles) and meteorological stations (blue-coloured triangles). The white rectangles surrounding the red circles and triangles represent the meteorological stations and the nearest grid station selected for the comparative analysis: **b)** Mean monthly temperature (T*max* and T*min*) and precipitation of the study area from 1980 to 2020: **c)** Annual peak discharge from 2003 to 2023 at three gauging stations of Jhelum basin namely, Asham, Sangam and Ram-Munshi Bagh.

Buri et al. 2022) and for comparative analysis with observed data in different parts of the world (Yin et al. 2015; Sidau et al. 2021).

In data-scarce regions like the Kashmir Valley, there is a sparse distribution of weather gauges, and access to extensive historical records of rainfall and temperature is restricted. Nevertheless, the existing observational data from the few available stations have been thoroughly examined to discern the annual, seasonal, and monthly trends in temperature and precipitation (Shafiq et al. 2019; Zaz et al. 2019; Ahsan et al. 2022; Romshoo et al. 2020; Ahmed et al. 2021; Dad et al. 2021; Lone et al. 2022). To conduct hydro-climatological investigations, long-term time series data is necessary (Sun et al. 2018). The availability of globally accredited high-resolution gridded rainfall datasets such as CHIRPS (1981-2020), APHRODITE (1951–2015), IMDAA (1970-2020), and CRU (1971-2020), as well as temperature datasets like APHRODITE (1951-2015), IMDAA (1970-2020), and CRU (1971-2020), provides an alternative resource for evaluating climate variability and trends across various global regions.

Any analysis based on temperature and precipitation is influenced by the resolution and temporal granularity of the spatial data products used (Wagner et al., 2012). Worldwide research on the validity of these gridded datasets has produced useful data for long-term evaluation of rainfall variability, even at a regional level (Singh and Xiaosheng 2019). However, the assessment of the long-term effects of rainfall and temperature at a higher resolution geographical scale is limited by their temporal and spatial availability. The details of the datasets used in this study, including their source, spatial resolution, and time series, are discussed in detail in the following sub-sections.

3.1.1. IMDAA

The Indian Monsoon Data Assimilation and Analysis (IMDAA) gridded dataset is a product of collaborative efforts among the National Centre for Medium-Range Weather Forecasting (NCMRWF) in India, the India Meteorological Department (IMD), and the UK Met Office (MO). This initiative is supported by the National Monsoon Mission (NMM) of the Ministry of Earth Sciences, Government of India. The IMDAA system is built upon the 4DVAR (four-dimensional variation) and its Unified Model (UM), developed by the Met Office. The system utilizes a sporadic cycle of data assimilation. The model domain encompasses areas beyond the Indian subcontinent that are crucial for the development of the Indian monsoon (Mahmood et al. 2018; Ashrit et al. 2020; Rani et al. 2021).

The IMDAA dataset, with a spatial resolution of 12.5 km, is available for access at https://rds.ncmrwf.gov.in/datasets. Specifically tailored for the Indian subcontinent and constructed using data from gauged stations and models, the IMDAA offers a highly precise and reliable record of observed rainfall, which is regarded as superior among global datasets. Rainfall measurements are provided in millimeters, and temperatures are recorded in Kelvin. The dataset spans from 1979 to the current period. It begins at a geographic coordinate of 6.5°N, 66.5°E, with subsequent data points such as 6.5°N, 66.75°E, and continues accordingly, with the final data point lying within the coordinates of 38.5°N and 100.0°E. The annual data file contains 365 or 366 records to accommodate both leap and non-leap years. More information about the datasets utilized in the study is available in Table 1 of the mentioned source (Pai et al. 2014).

Table 1. Data sources.

S. No.	Dataset Name	Resolution (km)	Time Frame	No. of Grid/Station	Source
1	CHIRPS	25	1981-2020	22	https://data.chc.ucsb.edu/products/CHIRPS-2.0/
2	IMDAA	12	1981-2020	22	https://rds.ncmrwf.gov.in/datasets
3	Aphrodite	25	1981-2015	22	http://aphrodite.st.hirosaki-u.ac.jp/product/
4	CRU	25	1981-2020	22	https://crudata.uea.ac.uk/cru/data/hrg/cru_ts_4.05/
5	Observed data	–	1981-2020	6	India Meteorological Department, Srinagar

3.1.2. CHIRPS

The Climate Hazards Group Infrared Precipitation with Station Data (CHIRPS) is a precipitation product derived from satellite observations that offers global rainfall datasets spanning 40 years. CHIRPS features high spatial and temporal resolution, integrating information from multiple sources. The CHIRPS V-2.0 rainfall datasets for the present study were acquired through the web link https://data.chc.ucsb.edu/products/CHIRPS-2.0/ hosted by the Climate Hazard Center, University of California. CHIRPS datasets are available in two spatial resolutions: 0.05°0.05° and 0.25°0.25°. In this study, CHIRPS data for 40 years from 1980 to 2020 was downloaded and extracted using Python software to analyze trends in climate variables. These datasets are extensively utilized for analysing trends and monitoring seasonal droughts (Funk et al. 2015; Paredes-Trejo et al. 2017; Sulugodu and Deka 2019).

3.1.3. APHRODITE

APHRODITE (Asian Precipitation - Highly-Resolved Observational Data Integration Towards Evaluation) offers a comprehensive set of daily continental-scale data products for Asia, which cover the years 1951 to 2015. This dataset includes detailed observations for regions such as the Himalayas, South and Southeast Asia, and mountainous zones in the Middle East. APHRODITE provides gridded climatological data solutions for a unified domain and four subdomains: Monsoon Asia, the Middle East, Russia, and Japan. The datasets offer a high-resolution daily record with a spatial resolution of either 0.25° x 0.25° or 0.05° x 0.05°, except for Japan, which consistently has a finer resolution of 0.05° x 0.05°. For Monsoon Asia, detailed daily mean precipitation and temperature data are available with a 0.05° x 0.05° resolution (Kamiguchi et al. 2010; Yasutomi et al. 2011; Hamada et al. 2012). APHRODITE's daily gridded precipitation dataset is unique as a long-term, continental-scale, high-resolution product. It incorporates data from an extensive network of 5,000 to 12,000 stations, which significantly exceeds the data typically provided by the Global Telecommunication System network by 2.3 to 4.5 times (Yatagai et al., 2012). While APHRODITE data generally performs exceptionally well across Asia, it is notably less representative in regions like the Tibetan Plateau (Ji et al. 2020). The dataset, spanning 35 years from 1980 to 2015, can be accessed through the provided link (https://climatedataguide.ucar.edu/).

3.1.4. CRU

The Climate Research Unit (CRU) time series offers a set of high-resolution gridded data, which has been widely utilized in historical studies for trend analysis across various regions (Grotjahn and Huynh 2018; Rao et al. 2018; Harris et al. 2020; Mutti et al. 2020). This dataset has a spatial coverage of a 0.5° latitude by 0.5° longitude grid, encompassing the entire global land surface except for Antarctica (Harris et al. 2020). The information provided is generated by interpolating monthly climatic anomalies using data from a comprehensive network of meteorological stations. The dataset has been updated as CRU TS v4, covering the time frame from 1901 to 2020, with additional station observations and annual updates (Harris et al. 2020). The creation of secondary variables has been altered to best fit this method, which now employs angular-distance weighting (ADW) as part of the interpolation process. In this study, gridded CRU temperature (Tmin, Tmax, and Tmean) and precipitation over 40 years from 1981 to 2020 was obtained from the Climate Research Unit of the University of East Anglia in the United Kingdom, available on their website at https://crudata.uea.ac.uk/cru/data/hrg/cru_ts_4.06/.

3.1.5. Observed data

Climate change and variability represent some of the most pressing issues confronting humanity today and have widespread consequences on the environment (Yu et al. 2019; Lee et al. 2023). Climate plays a significant role in people's lifestyles, means of subsistence, and overall socioeconomic development. Analysing observational meteorological data for a specific location over a period is one of the best methods to understand the climate of a place or region. To detect changes or variations in climate variables like temperature, precipitation, humidity, and wind across various time scales, conducting a trend analysis of climate data over the least 30 years is generally adequate for assessing the long-term impacts of a changing climate (Guan 2009). The observed temperature and precipitation records of the Jhelum basin, available at six meteorological stations namely Shalimar (Srinagar), Kupwara, Pahalgam, Kokernag, Gulmarg, and Qazigund, have been collected from the regional station of the India Meteorological Department located in Srinagar (Table 2).

The study analysed the annual trends in mean, minimum, and maximum temperature, as well as precipitation, on a station-by-station basis and for the entire Jhelum basin over 40 years from 1980 to 2020 (Table 1). The primary objective of this study was to analyse temperature and precipitation trends and compare the gridded datasets with the observed data. To achieve this, the annual trends of T*min*, T*max*, T*mean*, and precipitation derived from the gridded datasets (CHRIPS, APHRODITE, CRU, IMDAA) from 1980 to 2020, except APHRODITE (1980-2015), were compared with the trends acquired from the station data. The trend is obtained by analysing the relationship between the two variables and their temporal resolution. The significance of the trend was derived through statistical methods such as the coefficient of determination R^2 and regression analysis.

3.2. Resampling

The satellite-based rainfall and temperature datasets used in the study are available for various time periods and come with different spatial resolutions. Therefore, for

Table 2. General information about the IMD stations.

S. No	Name	Latitude (N)	Longitude (E)	Elevation (m)	Mean annual Temperature (°C)			Mean annual Precipitation (mm)
					Max	Min	Mean	
1	Srinagar	34° 03′	74° 48′	1588	19.64	6.80	13.22	813.21
2	Kupwara	34° 25′	74° 18′	1609	20.10	6.26	13.18	1082.87
3	Pahalgam	34° 02′	75° 20′	2310	16.88	3.27	10.07	1259.53
4	Kokernag	33° 40′	75° 17′	1910	18.17	6.52	12.35	1056.42
5	Qazigund	33° 35′	75° 05′	1690	19.28	6.40	12.86	1211.12
6	Gulmarg	34° 03′	74° 24′	2705	14.25	2.52	8.38	1332.41

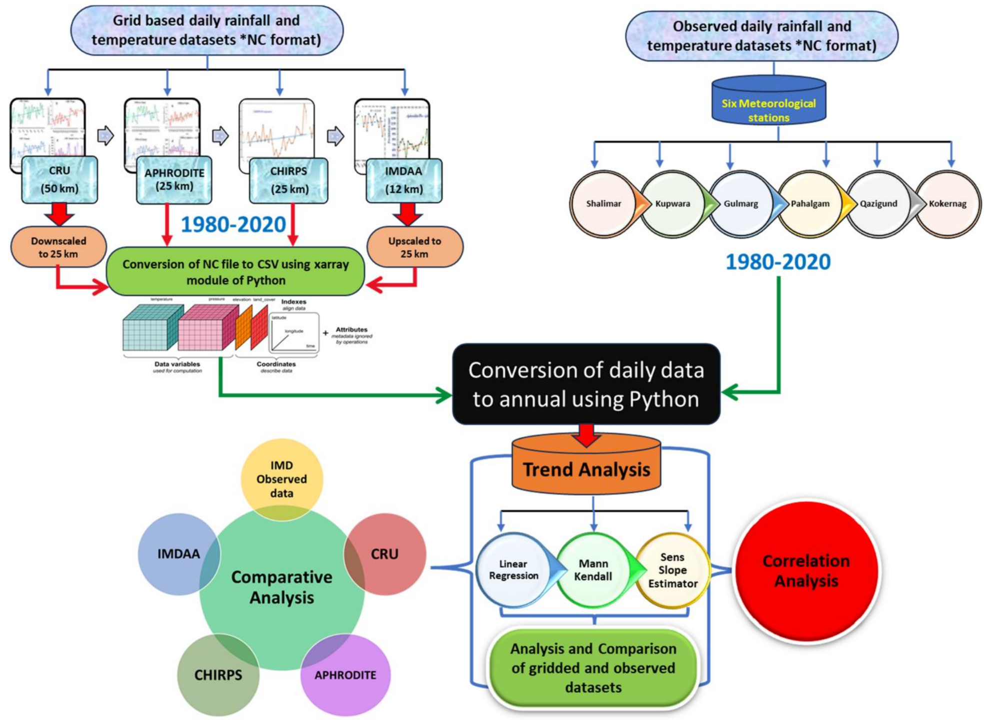

Figure 2. Flow chart of the methodology used in the study.

comparison and evaluation of the datasets, homogeneous series were prepared for a common time period (1981–2020) for IMDAA, CHIRPS, and CRU. However, APHRODITE is only available up to the year 2015, so the time period from 1981-2015 was considered. Additionally, all datasets were available at a resolution of 0.25° × 0.25°, except for IMDAA (0.12°×0.12°) and CRU (0.5°×0.5°). The IMDAA dataset was upscaled, and the CRU dataset was downscaled to 0.25° × 0.25° resolution using the nearest neighborhood interpolation method in the Python environment. The datasets were also examined for any gaps. The analysis revealed that there were almost no gaps present in the data sets used in this study for the selected time period (Figure 2).

3.3. Trend analysis

3.3.1. Mann-Kendall test

The Mann-Kendall trend test is an effective analytical tool for scrutinizing temperature and precipitation trends using observational data from six weather stations in the Jhelum basin of the Kashmir Himalayas, and for comparing these observations with assorted gridded datasets. This non-parametric test, which Mann introduced in 1945 and Kendall enhanced in 1975, is designed to detect trends in key environmental variables such as streamflow, temperature, and precipitation. These elements are essential to watershed modeling, a process that examines the characteristics of a catchment area to create sustainable water resource management strategies, as noted by Kothawale and Kumar in 2005. Ideal for research involving multiple data sources, the Mann-Kendall test has a proven track record in identifying climate variable trends at different scales, as documented by Yadav et al. (2014), Almazroui (2020), Zaz et al. (2019), Nourani et al. (2018), Ahsan et al. (2022), and Dad et al. (2021). In the current study, this test has been deployed to analyze and confirm statistically significant trends in climate data. The Mann-Kendall Statistic S for trend is:

$$S = \sum_{i=1}^{n-1} \sum_{j=i+1}^{n} sgn(x_j - x_i) \tag{1}$$

here, x_i, x_j are the sequential data values, whereas n is the length of the data set and

$$sgn(t) = \begin{cases} 1, & for\ \ t > 0 \\ 0, & for\ \ t = 0 \\ 1, & for\ \ t < 0 \end{cases} \tag{2}$$

In the Mann-Kendall trend test, the 'S' statistic is indicative of the trend's direction. A negative 'S' value denotes a decreasing trend, whereas a positive 'S' suggests an upward trend (Pal et al. 2017). Mann-Kendall has established that when $n \geq 8$, the 'S' statistic follows an approximate normal distribution, with specific mean and variance values as follows:

$$\mathrm{E(S)} \ = \ 0 \tag{3}$$

$$Var(S) = \frac{n(n-1)(2n+5) - \sum_{i=1}^{m} t_i(t_i - 1)(2t_i + 5)}{18} \tag{4}$$

The standardized test statistics Z is computed as follows.

$$Z_{MK} = \begin{cases} \dfrac{S-1}{\sqrt{Var(S)}}, & for\ \ S > 0 \\ 0, & for\ \ S = 0 \\ \dfrac{S+1}{\sqrt{Var(S)}}, & for\ \ S < 0 \end{cases} \tag{5}$$

In equation (5), m denotes the number of tied groups and the size of the ith tie group. The Z value is used to determine whether a statistically significant trend exists. A positive (negative) Z value indicates an upward (downward) trend. The Z_{MK} score, which is distributed normally, indicates the direction of a trend: an increasing trend for a positive Z_{MK} and a decreasing trend for a negative Z_{MK}. A trend in the data is considered statistically significant if the Z_{MK} value is beyond the critical value for the chosen significance level Z_{MK} Z/2. The Mann-Kendall test is designed to test the null hypothesis, which assumes there is no discernible trend in the dataset, against the alternative hypothesis that posits a trend is present (Kumar et al. 2013). This test's formula is applicable when there are 10 or more data points.

3.3.2. Sen slope estimator

The method of slope estimation put forth by Sen (1968) offers another non-parametric approach for conducting trend analyses on hydroclimatic data. It's particularly used to ascertain the extent of trends within climatic data, quantifying the degree of change over time by determining the slope's magnitude, under the presumption of a linear trend. This technique can be utilized to infer trends using univariate time series analysis. The Sen slope estimator offers a more accurate representation of trends in time series datasets due to its ability to remain insensitive to outliers and missing data (Sen, 1968; Duhan and Pandey 2013). In this study, the Sen slope estimator has been used, and subsequently, a test has been performed using Python 3.9.

$$T_i = \frac{X_j - X_k}{j - k} \quad for \ i = 1, 2, 3, \ldots, N \tag{6}$$

In equation (6), X_j and X_k represent data values at times j and k respectively, within a given time series, where j > k. The slope between each pair of data points is calculated to determine the rate of change. The Sen's Slope estimator is then derived by taking the median of all these calculated slopes from the N observations as:

$$\begin{aligned} Q_i &= T_{\frac{N+1}{2}} \quad for \ N \ is \ odd \\ &= \frac{1}{2}\left(T_{\frac{N}{2}} + T_{\frac{N+1}{2}}\right) for \ N \ is \ even \end{aligned} \tag{7}$$

The Sen slope estimator is calculated as Qmed = $(N+1)/2$ when the N slope data are displayed as odd and as Qmed = [(N/2) + $((N+2)/2)$]/2 when the N slope observations are shown as even.

The estimate of the slope is the median of these N values of Q. If each time period only contains one datum, then N' = n (n − 1)12, where n is the total number of time periods. Two independent confidence intervals are produced by the process in the VB macro, which generates two separate confidence intervals = 0.01 and = 0.05. Using the non-parametric process proposed by Sen (1968), a 100 (1%) two-sided confidence interval around the true slope can be determined (Mondal et al. 2012). The positive or negative slope Qi is attained as an upward or downward trend that represents the decreasing and increasing trend in the time series.

3.3.3. Regression analysis

The regression analysis method is a parametric approach that is applied to ascertain whether a dataset follows a normal distribution (Radhakrishnan et al. 2017). In this technique, time (x) is taken as an independent variable, whereas climate variables (y) are taken as dependent variables to analyze the linear trend. The regression line is employed to characterize the trend patterns in climatic variables (temperature and precipitation) at various levels, such as monthly, seasonal, annual, and decadal, tailored to the specific objectives of the research study. Equation (8) was used to analyze the annual trend of climate variables from 1980 to 2020. The regression formula is:

$$Y = a + bx \tag{8}$$

Where 'x' and 'y' in equation (8) represent the independent and dependent variables, respectively while 'a' represents the intercept and 'b' represents the slope.

3.3.4. Correlation analysis

Understanding the correlation between variables is essential for statistical modelling, as highlighted by various researchers such as Gong et al. (2017) (Chambers and Hastie, 2017), and Yan et al.(2021) . According to Zaki et al. (2020), Chatterjee and Rangarajan (2022), and Steger et al. (2021), correlation analysis is a descriptive tool that is frequently utilized and beneficial in this setting for studies of this kind. Karl Pearson's correlation coefficient, which is generally accepted for its reliability in capturing linear correlations, was employed to evaluate the interdependence of the variables in our investigation.

$$r = \frac{\sum_i^n \left(X_i - \overline{X}\right)\left(Y_i - \overline{Y}\right)}{\sqrt{\sum_i^n \left(X_i - \overline{X}\right)^2} \cdot \sqrt{\sum_i^n \left(\mathrm{Y}_i - \overline{\mathrm{Y}}\right)^2}} \tag{9}$$

Where Xi and Yi represent the ith occurrence of variables X and Y from an n-sample, X and Y are the sample means of the two variables. The value of r can range between −1 and +1. When $r = 0$, it means that there is no connection between the variables of interest. In contrast, r0 shows that an increase in one variable causes a reduction in the value of another, implying that the variables have a negative relationship. On the other hand, a condition where $r > 0$ shows that a rise in one variable induces an increase in the value of another variable, which is known as a positive correlation. Conditions in which r approaches 1 imply that there is a strong association between the variables of interest.

Our examination focused on the relationship between observed P and Z values for gridded and observed T*max* and annual precipitation. The identified effectiveness of Karl Pearson's coefficient of correlation in measuring linear relationships between variables led to its selection. This technique has been frequently used in similar scenarios, offering a reliable and well-known tool for examining relationships within the datasets being studied. By using this statistical technique, our correlation analysis becomes more credible and robust, leading to a deeper understanding of the complex relationships between the variables in our study.

4. Results

The annual average trends of climate variables such as temperature (T*max*, T*min*, and T*mean*) and precipitation were derived for both gridded and observed data using the Mann-Kendall test and Sen slope estimator at a 95% confidence level. 'P' and 'Z' values were generated for Tmax, T*min*, T*mean*, and Precipitation (annual mean).

After processing the gridded data for the Jhelum basin, a .csv file with 22 grids was generated. We present the results in three sections. Firstly, temperature and precipitation trends in gridded datasets are examined across the Jhelum basin. Secondly, the temperature and precipitation trends are analyzed for all 6 meteorological stations: Shalimar, Qazigund, Kokernag, Pahalgam, Gulmarg, and Kupwara. Thirdly, the annual average trends for the gridded datasets and observed data are compared. The following results represent the annual average trend analysis for both gridded and observed temperature and precipitation data across the Kashmir Valley.

4.1. Annual average temperature and precipitation trends (grided datasets)

4.1.1. IMDAA trends

The Mann-Kendall test has been utilised to IMDAA-based minimum (T*min*), maximum (T*max*), and mean (T*mean*) temperatures. All the temperatures show increasing trends with $Z > 0$. The P and Z-values for T*max*, T*min*, and T*mean* are given in Table 3. In the IMDAA gridded data, the average T*max* of the Jhelum basin is 13.18 °C during the period from 1981 to 2020. The average change in T*max* per year is found to be 0.028 °C/year. The highest T*max* was found in the year 2016 (14.94 °C), and the lowest T*max* was in the year 1986 (11.47 °C). On the other hand, the average T*min* for the same period is 2.27 °C. The average change in T*min* per year is found to be 0.035 °C/year. The highest T*min* (3.32 °C) was in the year 2020, whereas the lowest T*min* (0.82 °C) was found in the year 1983. Overall, all three temperature scenarios, i.e. T*max*, T*min*, and T*mean*, revealed increasing trends in the study region as depicted in Figure 3a–c. The Mann-Kendall Test for the IMDAA dataset's mean annual precipitation demonstrated a statistically significant decreasing trend with a z-statistic value of < 0. According to the IMDAA gridded dataset, the average annual precipitation is 1690 mm, and the average annual precipitation rate is −5.07 mm per year from 1981 to 2020. The highest annual precipitation (2342 mm) was recorded in 1992, and the lowest precipitation (1165 mm) was in 2004 (Figure 3d). The P and Z values for average annual precipitation in each grid on the monthly time scale are presented in Table S1.

4.1.2. CRU trends

The trends in T*max*, T*min*, T*mean*, and mean annual precipitation derived from the CRU data are depicted in Figure 4. The Mann-Kendall test has been applied to CRU-derived maximum (T*max*) and minimum (T*min*) temperature data from 1981 to 2020. Both the maximum and minimum temperature records exhibit an upward trend with Z-values >0 (Figure 4a and b). Similar to the IMDAA data, the Mann-Kendall analysis of the mean annual temperature (T*mean*) from the CRU dataset also demonstrates a statistically significant increasing trend with a P value >0.01 and a Z value of 3.7, which underscores the high significance of the trend noted.

The analysis of the mean annual maximum temperature (T*max*) for the period 1981 to 2020 indicates an average T*max* of 12.14 °C. The highest T*max* (12.96 °C and 12.98 °C) is found in the years 1999 and 2016, whereas the lowest T*max* (11.26 °C) is found in the year 1983 (Figure 4a). The mean annual T*max* rate is 0.02 °C per year.

Table 3. Descriptive statistics for maximum, minimum and mean temperatures and precipitation.

	Maximum Temperature				Mean Temperature				Minimum Temperature				Annual Precipitation			
Stations	Trend	P-Value	Z-Value	Sen Slope	Trend	P-Value	Z-Value	Sen Slope	Trend	P-Value	Z-Value	Sen Slope	Trend	P-Value	Z-Value	Sen Slope
Shalimar	Increasing	0.003	2.93	0.043	Increasing	0.014	2.43	0.02	No	0.72	−0.34	−0.002	No	0.5	−0.674	−1.86
Qazigund	No	0.138	1.48	0.018	No	0.08	1.71	0.014	No	0.27	1.08	0.005	No	0.196	−1.29	−5.2
Kokernag	Increasing	0.005	2.75	0.04	Increasing	0.0014	3.19	0.03	Increasing	0.032	2.13	0.016	No	0.56	−0.57	−1.74
Pahalgam	Increasing	0.0001	3.8	0.055	Increasing	2.24	5.17	0.05	Increasing	3.21	5.11	0.05	No	0.16	−1.38	−5.15
Gulmarg	No	0.597	0.52	0.14	No	0.16	1.39	0.03	No	0.12	1.55	0.02	No	0.08	−1.69	−7.06
Kupwara	Increasing	0.0014	3.19	0.04	No	0.01	2.54	0.023	No	0.49	0.68	0.007	No	0.167	−1.38	−1.38

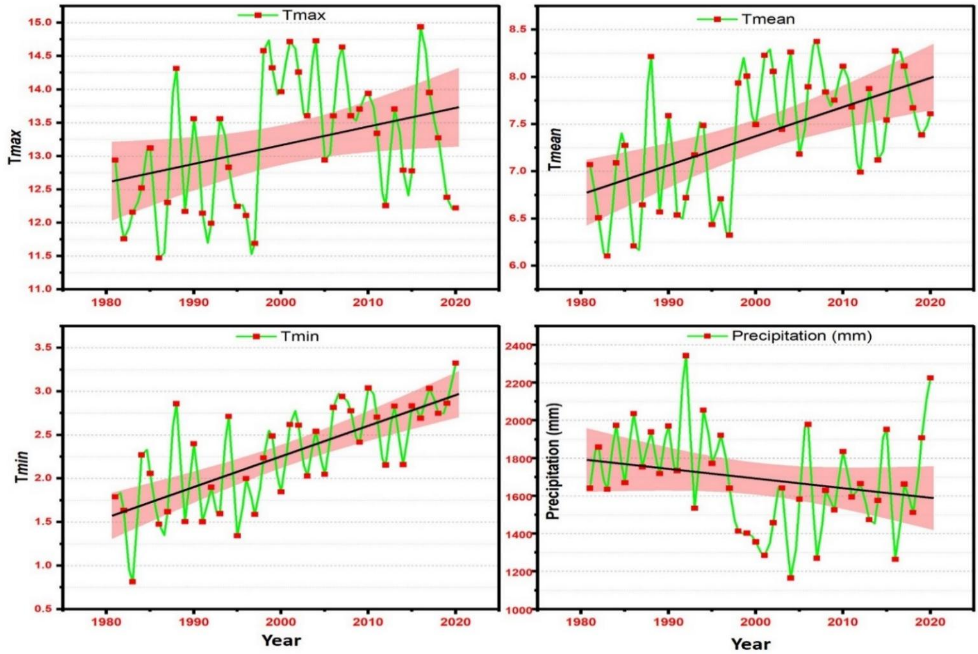

Figure 3. Annual average temperature and precipitation of the Jhelum basin from 1981 to 2020 derived from the IMDAA. The black line represents the linear trend.

Similarly, the mean T*min* is 1.56 °C, with an annual T*min* rate of 0.037 °C per year (Figure 4c), showcasing a notable rise in the mean temperatures for the region (Figure 4b). The CRU precipitation data analysis reveals that the average precipitation of the Jhelum basin is only 678 mm. The annual precipitation change is positive, i.e. it has increased by 2.9 mm per year (Figure 4d).

4.1.3. APHRODITE mean annual temperature precipitation trends

The analysis of the mean annual temperature (T*mean*) derived from the Aphrodite dataset reveals an increasing trend with a Z value of 1.36. The mean annual temperature (T*mean*) in the Jhelum basin over the 1981-2015 period is 7.92 °C. The change rate in Tmean is 0.022 °C per year (Figure 5a). Similarly, the annual precipitation derived from the Aphrodite dataset also reveals an increasing trend, like the CRU gridded dataset, at 10 mm per year. The average annual precipitation in the Jhelum basin for the 1981 to 2015 period is 805 mm (Figure 5b). It also reveals that the highest annual precipitation of 1411 mm occurred in 2011, and the lowest annual precipitation of 456 mm occurred in 2000.

4.1.4. Precipitation trends from the CHIRPS dataset

The CHIRPS dataset also revealed an increasing trend, like the CRU and APHRODITE datasets, in annual precipitation with a P value > 0.01 and Z statistic values > 0. According to the CHIRPS gridded dataset, the average annual precipitation in the Jhelum basin over the 1981-2020 period is only 563 mm (Figure 6). The lowest annual mean precipitation (310 mm) was recorded in 2000, while the highest

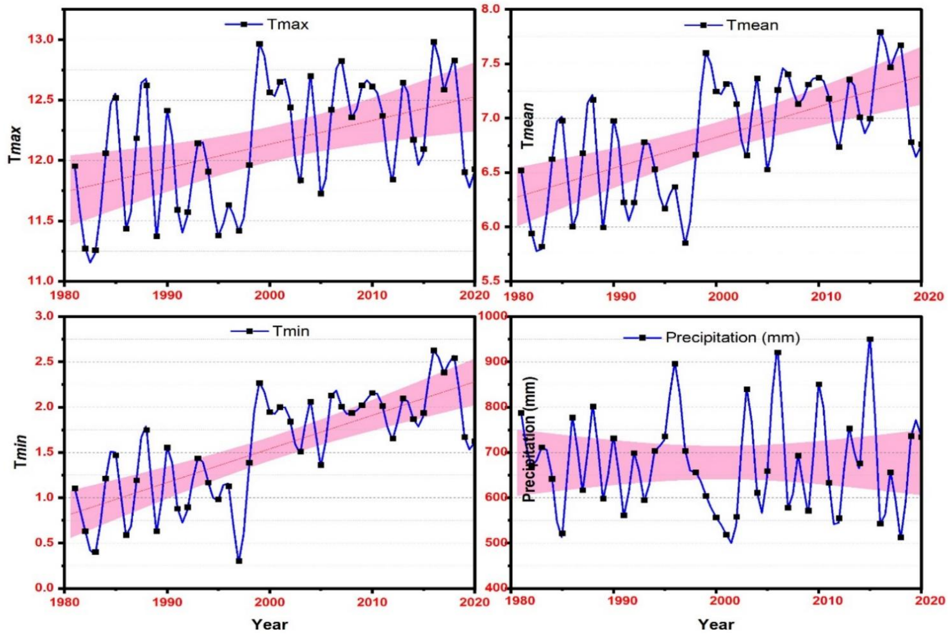

Figure 4. Annual average temperature and precipitation of the Jhelum basin from 1981 to 2020 derived from the CRU. Red line line represents the linear trend.

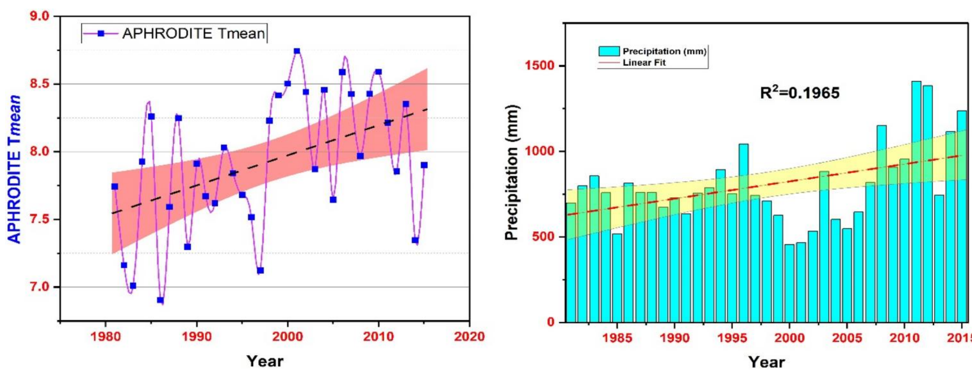

Figure 5. Trends from Aphrodite dataset **(a)** T*mean* **(b)** Mean annual precipitation. Dashed lines represent linear trend.

annual mean precipitation (998 mm) was observed in 2014 (Figure 6). The average annual precipitation is found to be increasing at a rate of 3.93 mm per year.

4.2. Overall trends in the gridded climate datasets

4.2.1. Precipitation trends

Tables S1 and S2 present the descriptive statistics calculated for trend analysis. The analysis of precipitation trends was conducted using satellite-based datasets, namely CHIRPS, CRU, IMDAA, and APHRODITE datasets, as mentioned in section 3. The CHIRPS dataset showed a non-significant increasing trend in precipitation, with an R^2 value of 0.11 and an increase rate of 3.93 mm per year (Figure 6). The CRU

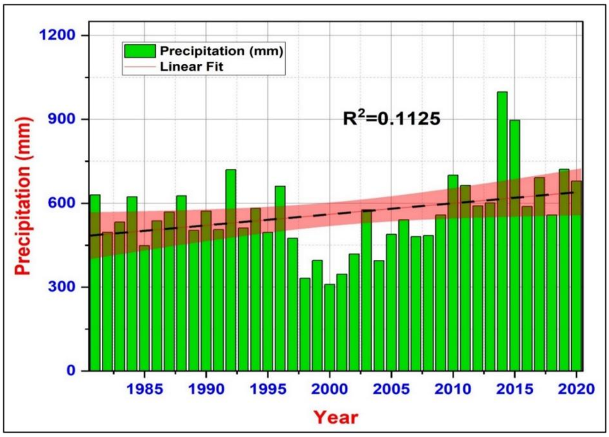

Figure 6. Precipitation trends from CHIRPS dataset.

dataset also indicated a non-significant but increasing trend, with precipitation increasing by 2.9 mm per year (Figure 4d). APHRODITE exhibited an overall increasing trend, with an R^2 value of 0.19 and an increase rate of annual precipitation at 10 mm per year (Figure 5b). On the other hand, IMDAA showed an overall non-significant but decreasing trend, with an R^2 value of 0.049 and annual precipitation decreasing at a rate of 5.07 mm per year (Figure 3d).

4.2.2. Temperature trends

Tables S1 and S2 provide the descriptive statistics for trend analysis. Satellite datasets, namely CRU, IMDAA, and APHRODITE, were used to analyze temperature trends for all three scenarios: T*max*, T*min*, and T*mean*. The CRU dataset showed an increasing trend in all three scenarios. The mean annual maximum temperature (T*max*) was 12.14 °C, and the minimum temperature (T*min*) was 1.56 °C during the 1981-2020 period. The annual T*max* rate was 0.02 °C per year, and the annual T*min* rate was 0.037 °C per year (Figure 4b). T*max* exhibited a significant increasing trend with an R^2 value of 0.20, T*mean* showed similar behavior with an R^2 value of 0.38, and T*min* showed a significant increase with an R^2 value of 0.53 (Figure 4a and c). For IMDAA, T*max* showed an increasing trend with an R^2 value of 0.21, and the average change in mean T*max* was 0.028 °C/year (Figure 3c). T*min* showed a significant decreasing trend with an R^2 value of 0.50, and the average change in mean T*min* per year was 0.035 °C/year (Figure 3b). Only T*mean* was available for the APHRODITE dataset, and it showed an increasing trend with a variability (R^2) of 0.23 and an average change rate of 0.022 °C per year (Figure 5a). The P, Z, and Sen Slope values of T*mean* for all the gridded datasets are provided in the Supplementary data (see Figure S7).

4.3. Temperature and precipitation trend analysis using observed data

For observed station data, all three temperature scenarios showed significant increasing trends. The average T*max* over the last four decades was 17.71 °C. T*max*

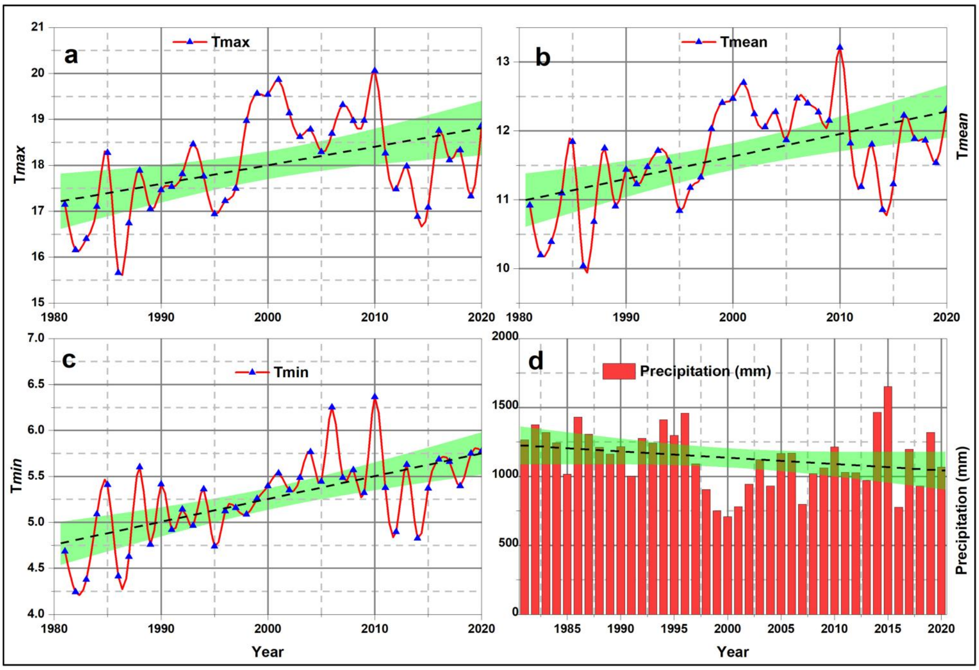

Figure 7. Trends in the recorded IMD data in the Jhelum basin.

exhibited an average increase rate of 0.024 °C per year with an R^2 value of 0.2 (Figure 7a). T*mean* showed a significant increasing trend with an R^2 value of 0.28 (Figure 7c). The average T*min* was 5.42 °C, and it increased at a rate of 0.015 °C per year with an R^2 value of 0.39 (Figure 7b). Regarding the precipitation scenario, the observed data indicated that the average annual precipitation in the Jhelum basin during the 1981-2020 period was 1138 mm, which showed a non-significant decrease at a rate of 3.36 mm per year (Figure 7d). The P, Z, and Sen Slope values of annual precipitation and T*mean* for all the observed stations are presented in the supplementary data (see Figure S8), while T*max* and T*min* are presented in Figure S9.

4.4. Temperature and precipitation trends: Station-wise analysis (1980-2020)

The analysis of long-term weather data from various stations in the Kashmir region provides valuable insights into the evolving climate trends over the past four decades, from 1981 to 2020. Beginning with the Shalimar (Srinagar) station (Table 3, Figure S1), significant trends are observed, particularly in maximum and minimum temperatures. The average maximum temperature demonstrates a noteworthy increase of 1.79 °C over the period, indicating a consistent warming trend at an annual rate of 0.04 °C. Conversely, the minimum temperature shows a declining trend, decreasing at an average annual rate of 0.02 °C. The mean temperature, derived from the combination of maximum and minimum temperatures, also registers a 0.7 °C increase over the 40 years. Additionally, a distinct declining trend in precipitation, albeit minimal, is evident, suggesting potential shifts in regional rainfall patterns.

At the Qazigund station (Table 3, Figure S2), although temperature trends show less pronounced changes compared to Shalimar, incremental shifts are noted. Maximum temperatures exhibit a slight rise, while minimum temperatures demonstrate a minor but upward trend. The mean temperature sees a modest increase over the period. However, precipitation trends indicate a significant decreasing trend, potentially signalling alterations in the region's precipitation dynamics.

At the Kokernag station (Table 3, Figure S3), significant increases are observed in both maximum and minimum temperatures, reflecting a clear warming trend over the past four decades. The mean temperature also shows a notable rise, albeit with less pronounced changes compared to individual temperature components. Despite these temperature shifts, precipitation trends show a slight, insignificant decrease, suggesting relatively stable rainfall patterns.

Moving forward to the Pahalgam station (Table 3, Figure S4), the warming trend becomes more pronounced, with significant increases noted in maximum, minimum, and mean temperatures. Maximum temperatures rise notably by 2.4 °C, accompanied by a substantial increase in minimum temperatures. The mean temperature also sees a significant rise of 2.6 °C over the period. Interestingly, despite these temperature shifts, precipitation trends remain relatively stable, indicating consistent rainfall patterns in the region.

At the Gulmarg station (Table 3, Figure S5), temperature changes are more subtle, with minor increases observed in both maximum and minimum temperatures. However, the mean temperature exhibits a noteworthy rise over the 40-year span. Precipitation trends indicate a slight decrease, though statistically insignificant, suggesting minimal changes in regional rainfall patterns.

Lastly, at the Kupwara station (Table 3, Figure S6), a significant increase in maximum temperature is observed, accompanied by slight upward trends in minimum and mean temperatures. Precipitation, on the other hand, displays a non-significant decreasing trend. These analyses collectively highlight the complex dynamics of climate change in the Kashmir region, emphasizing the need for continued monitoring and adaptive measures to address potential impacts effectively.

Several studies, such as Ahsan et al. (2022), Shafiq et al. (2019), and Zaz et al. (2019), observed warming trends in the Kashmir region using observed data from the India Meteorological Department (IMD). Ahsan et al. (2022) reported a T*max* increase of 0.034 °C/year with an R^2 of 0.12 and a T*min* increase of 0.016 °C/year with an R^2 of 0.05, while Shafiq et al. (2019) recorded slightly lower increases in T*max* (0.03 °C/year) but a higher R^2 value of 0.22. These studies also noted significant decreases in precipitation, with Ahsan et al. reporting a reduction of −5.73 mm/year and Shafiq et al. reporting −7.07 mm/year. In contrast, studies focusing on the Upper Indus Basin (UIB) like those by Fowler and Archer, 2006 and Archer et al. (2004) observed negligible changes in maximum and minimum temperatures but slight increases in mean temperature, as indicated by Fowler et al. (2006) with a T*mean* increase of 0.02 °C/year and R^2 of 0.04. Archer et al. (2004) found no significant temperature trend but reported a minor positive precipitation trend. Ren et al. (2014) and Garg et al. (2019) investigated the broader Hindukush and Eastern Himalayan regions, respectively, revealing more pronounced warming trends. Ren et al. reported a T*max* increase of 0.08 °C/year in the Hindukush Himalayas, while Garg et al. documented a 0.04 °C/year increase in T*max* and 0.03 °C/year in T*min*, along with a slight increase in T*mean* and stable precipitation trends (See Table S4). The present study, comparing observed data and gridded data for the Kashmir region, found a T*max* increase of 0.024 °C/year using observed data and varying results with gridded datasets. The gridded data from IMDAA showed the highest T*max* increase (0.028 °C/year) compared to other datasets, with a corresponding precipitation decrease of −5.71 mm/year. Gridded data from APHRODITE, CHIRPS, and CRU also revealed differing temperature and precipitation trends, with the APHRODITE dataset showing a significant precipitation increase of 10 mm/year. Our study aligns with previous research, indicating a consistent warming trend in the Kashmir region, with a T*max* increase of 0.024 °C/year and a T*min* increase of 0.015 °C/year, similar to findings by Ahsan et al. (2022) and Shafiq et al. (2019). However, our observed precipitation decrease of −3.36 mm/year is less severe than in some studies, while gridded data from APHRODITE suggests an unexpected increase in precipitation. This discrepancy between observed and gridded data highlights the variability in climate trends across different sources, underscoring the complexity of regional climate dynamics.

5. Discussion

Gridded datasets are an important source of meteorological data for various hydrometeorology climate change studies, particularly in regions characterised by limited availability and inadequate coverage of observatory stations. This study utilized meteorological parameters of temperature and precipitation from the gridded datasets (APHRODITE, CHIRPS, CRU, and IMDAA) and observed climate datasets from the Indian Meteorological Department. This study is probably the first of its type and represents a pioneering effort in investigating the climatic fluctuations within the Jhelum basin by employing a diverse range of gridded climate data products. Furthermore, a comparative examination of these datasets was undertaken, followed by validation through observed station data. The main goal of this research is to determine the degree of bias present in different gridded datasets generated by different organizations, and subsequently identify the most reliable gridded data product suitable for regions with limited data availability in the North Western Himalayas. It identifies trends in temperature and precipitation (presented in Table 3 and Supplementary Tables S1 and S2) in each of the gridded datasets for 22 grid points and 6 meteorological stations located in the Jhelum basin. The grid point-based temperature and precipitation trends are given in Figures 8 and 9. The comparative examination of temperature and precipitation trends in the Kashmir Himalayas, based on observed and gridded datasets, has yielded insightful findings that contribute to our understanding of regional climate dynamics. Our study revealed a notable increase in mean annual temperatures (T max, T min, and T mean) across the region over the 1981–2020 period, aligning with global climate change trends reported in various studies (Bloomfield 1992; Folland et al. 2001).

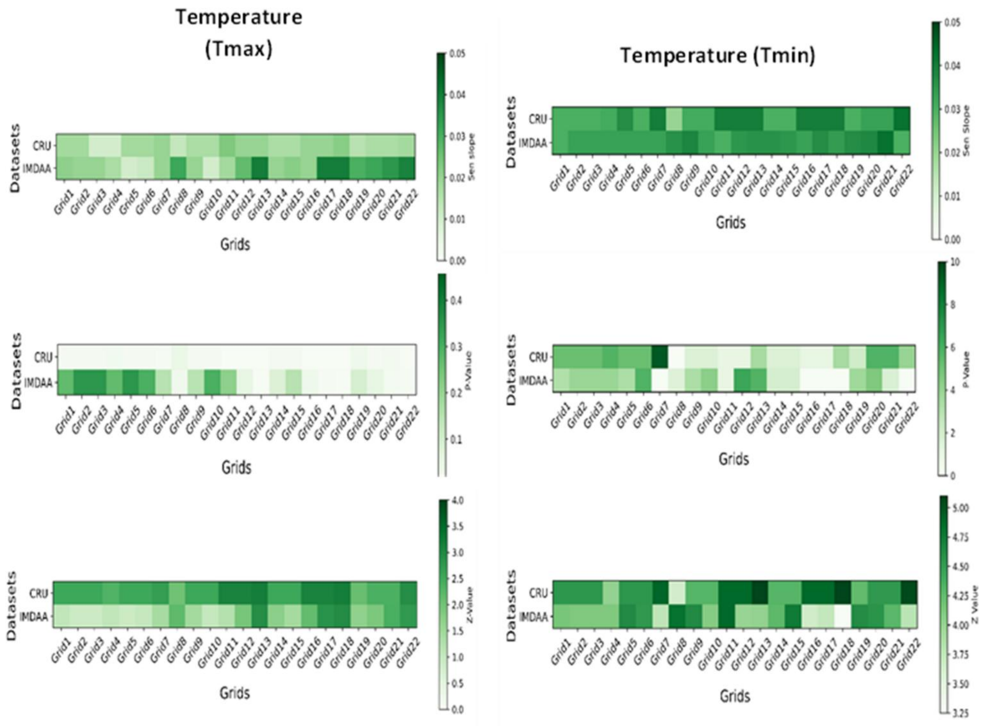

Figure 8. Grid point based-temperature trends of gridded datasets.

The observed mean annual T*max* and T*min* show net increases of 1 °C and 0.62 °C, respectively. The T*mean* also shows an increase of 0.9 °C. These increasing rates are consistent with other local studies (Shafiq et al., 2019; Zaz et al. 2019; Ahmed et al., 2022; Mir et al. 2024). Among the gridded datasets, although CRU shows similar net increases in T*max* (1 °C) and T*min* (1.6 °C), it underestimates the magnitude of T*max* and T*min* by approximately 5 °C and 4 °C. In APHRODITE, only the T*mean* is available, and it shows an increase of about 1 °C (from 7.5 °C to 8.5 °C), thus underestimating the actual observed T*mean* change from 11.1 °C to 12 °C. In IMDAA gridded data, although both T*max* and T*min* increased from 12.6 °C to 13.7 °C and 1.6 °C to 2.9 °C, respectively, these values also underestimate the actual observed temperature variables for most of the stations by around 6 °C and 3 °C. Therefore, it can be concluded that all gridded datasets considered show increasing trends in temperature, aligning with the direction of trends in observed temperature. IMDAA, which has proven to be the best available gridded data product for this study, indicates the least differences (2 °C to 4 °C) with respect to observed temperatures in areas with relatively low altitudes (Srinagar, Kokernag, and Qazigund), and higher differences in areas with higher altitudes (Gulmarg and Pahalgam). In Pahalgam, IMDAA underestimates T*max* by 11 °C and T*min* by 6.5 °C. In the case of Gulmarg, IMDAA overestimates T*max* by 4 °C and T*min* by 1.5 °C, respectively. The meteorological stations and subsequent grid points-based

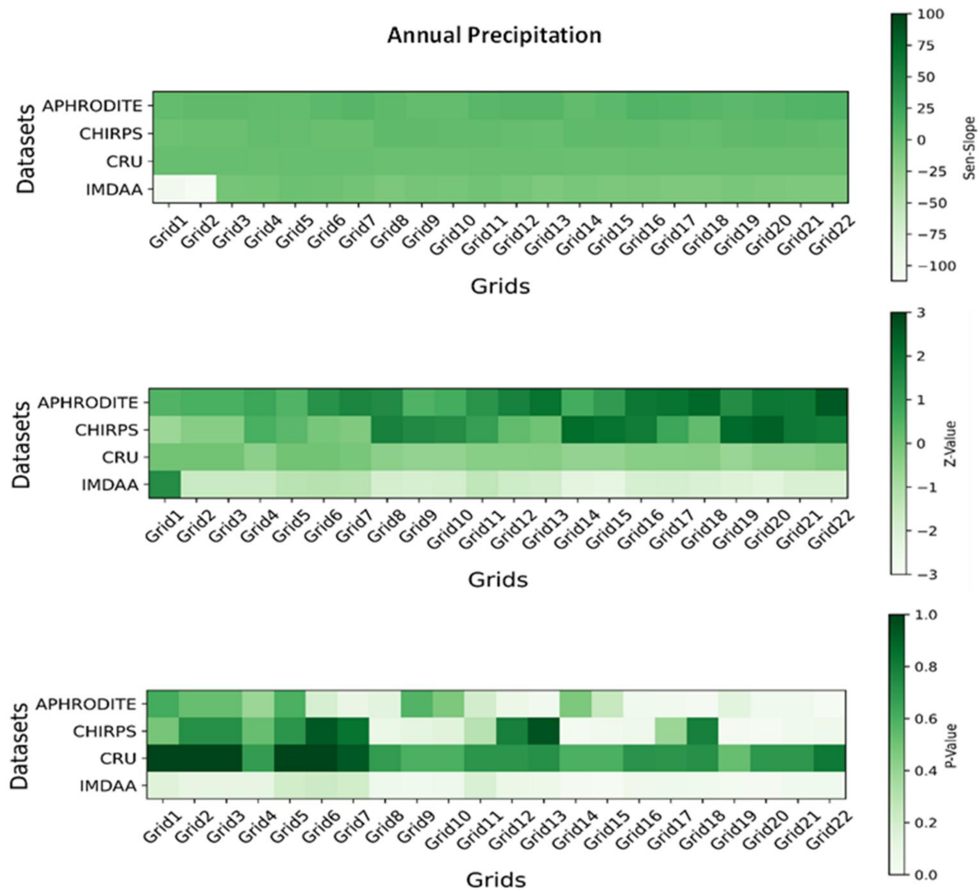

Figure 9. Grid point-based precipitation trends of gridded datasets.

comparison graphs of observed and IMDAA temperatures and precipitations are provided in Figures 10 and 11.

The mean annual precipitation in the Jhelum basin from 1981 to 2020 stands at 1138 mm, with a slight, insignificant decrease of 3.36 mm per year. It has decreased from 1266 mm to 1068 mm (198 mm) in the Jhelum basin in 40 years. In contrast, among the gridded datasets, the CHIRPS gridded dataset shows an average annual precipitation in the Jhelum basin over the period 1981-2020 of only 563 mm, exhibiting an increase of 160 mm from 490 mm to 650 mm. This not only presents an opposite or increased trend rate of 3.93 mm per year but also inaccurately shows only half of the actual observed precipitation. In CRU, the average precipitation of the basin is 678 mm, increasing at 2.9 mm per year. In APHRODITE, the average annual precipitation is 805 mm, showing an increasing trend of 10 mm per year. On the other hand, IMDAA reveals a decrease in precipitation from 1800 mm to 1600 mm, which is similar to the observed decrease of 198 mm, but even the gridded dataset of IMDAA overestimates the observed precipitation. The precipitation trends at each grid point are presented in Figure 9.

There are noticeable variations in the observed changing precipitation rates, with 5 out of 6 stations showing decreasing precipitation rates ranging from −0.1 mm per

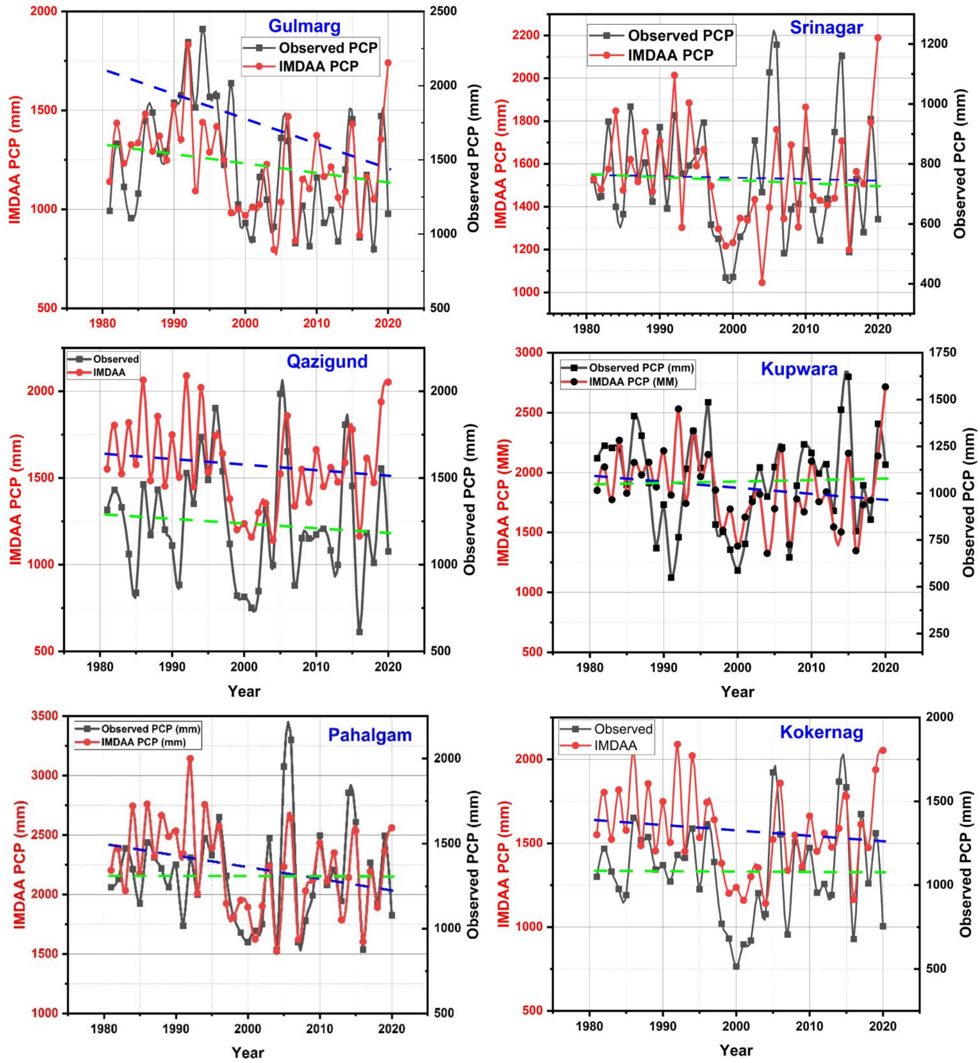

Figure 10. Comparison of linear trends between observed and IMDAA annual precipitation.

year in Pahalgam to −12.5 mm per year in Gulmarg. Only Kupwara shows an insignificant increase in precipitation at 0.7 mm per year, highlighting the influence of local topography and microclimatic conditions on climate trends. Similarly, the gridded datasets exhibited decreased precipitation rates for all stations but showed much differences in comparison to the observed precipitation at the elevated stations such as Gulmarg and Pahalgam. Thus, the IMDAA gridded data shows more discrepancies for hill stations. Moreover, our analysis identified a decline in annual precipitation at a rate of 3.36 mm per year based on observed precipitation records. This declining trend is consistent with previous studies conducted in the Jhelum basin (Zaz et al., 2019; Ahmad et al., 2022; Ahsan et al. 2022; Ahmed et al., 2022; Wani et al. 2022; Lone et al. 2022). However, most of the gridded datasets painted unreal precipitation scenarios and mostly identified increased precipitation trends over the

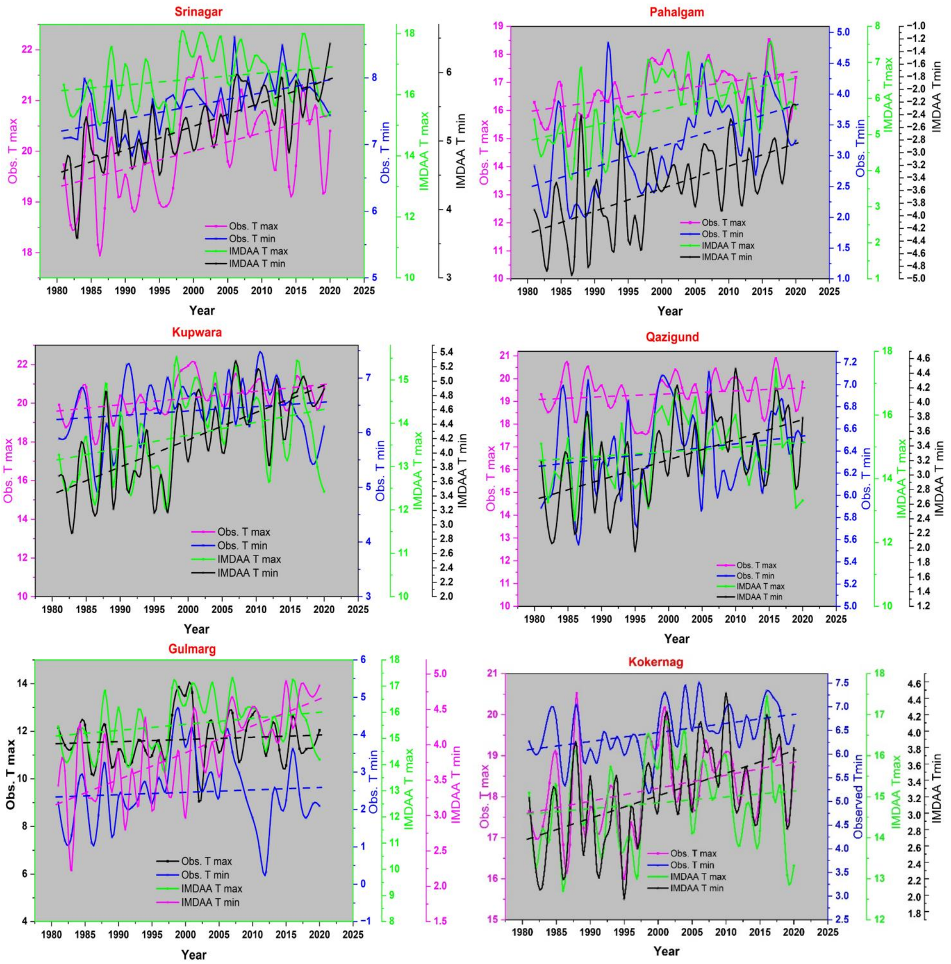

Figure 11. Comparison of linear trends between observed and IMDAA Tmax and Tmin at six stations.

Jhelum basin. In contrast, the IMDAA gridded dataset, which is the gridded dataset of the Indian Meteorological Department, is an exception as it accurately shows the direction and magnitude of the decreased precipitation trend, but it over-represents the absolute annual precipitation of the basin by about 30%. The observed and IMDAA precipitation comparisons for each station are presented in Figure 10.

This emphasises the necessity of exercising caution when exclusively relying on gridded datasets for evaluating precipitation in complex topographies like the Himalayas. It is preferable that gridded datasets undergo bias correction by utilising reliable observed data as a benchmark. Gridded datasets should also investigate the factors driving elevation-dependent temperature changes and refine precipitation modelling approaches to better capture the nuances of ecologically sensitive areas like the Jhelum basin. This study also emphasizes the importance of integrating both observed and gridded datasets to gain a comprehensive understanding of climate variability in areas with limited climate data.

Our research offers valuable insights for the comparison of gridded climate datasets in the Jhelum Basin of the North-western Himalayas. However, it is crucial to acknowledge certain significant limitations. In particular, the complex topography of the Himalayas poses challenges, particularly at elevated altitudes where disparities in gridded datasets become more pronounced. These variations underscore the necessity of exercising caution when solely relying on gridded data in regions with such complex terrains. Each gridded dataset has its own unique constraints. For example, CRU underestimates temperature magnitudes and APHRODITE underrepresents changes in T*mean*. These dataset-specific problems emphasize the importance of carefully selecting an appropriate dataset for analysis. Considering these constraints, several suggestions are made for future studies. In challenging environments like the Himalayas, advanced bias correction techniques should be investigated and used to improve the accuracy of gridded datasets, correcting anomalies, and enhancing their reliability. Integration of satellite-derived data may also provide insightful information on climatic variables to enhance gridded datasets and observed data for a more comprehensive understanding of climate dynamics.

Conducting localized validation activities that compare high-quality observed data at specific locations with gridded datasets is of utmost importance within an academic context. This methodology serves to identify and resolve any limitations within the datasets, particularly in areas characterized by complex topography. Further research should focus on delving into the complex climatic dynamics of the Himalayas, with a specific emphasis on evaluating the efficacy of gridded datasets in capturing regional variations in temperature and precipitation. It is crucial to prioritize enhancing precipitation modelling techniques within gridded datasets, especially in locations with diverse topography, to address existing research gaps. Furthermore, exploring the integration of different gridded datasets with observed data holds immense potential for the development of hybrid datasets that effectively combine the strengths of each dataset while mitigating their limitations. Adopting this integrated approach has the potential to yield more accurate climate assessments and enhance our comprehension of climate variability in regions with limited data availability.

5.1. Correlation analysis

The correlation coefficients and corresponding p-values between the four gridded precipitation datasets - APHRODITE, IMDAA, CHIRPS, and CRU - and the observed station data are displayed in Figure 12. Strong positive correlations (0.8) with APHRODITE, IMDAA, and CHIRPS, moderate negative correlations (-0.23) with CHIRPS, and very weak positive correlations (0.04) with CRU have been observed in the observed data. APHRODITE exhibits positive correlations with CRU (0.42) and IMDAA (0.19) among the gridded datasets, and a modest positive connection with CHIRPS (0.06). IMDAA and CRU show a similar amount of positive correlation (0.38), whereas IMDAA and CHIRPS show a moderate positive association (0.33). The correlation between CHIRPS and CRU is strongly positive (0.63). The p-values of these correlations offer details about their statistical significance. Lower p-values indicate that there is more evidence against the null hypothesis of no link.

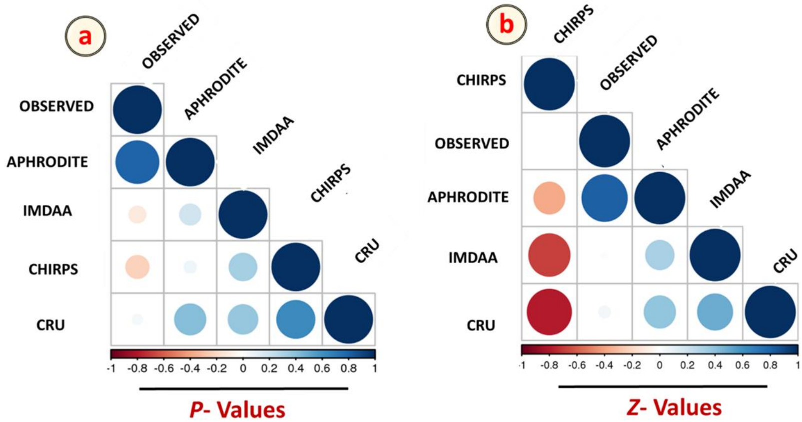

Figure 12. Pearsons's correlation between gridded and observed datasets **a)** P-value b) **Z**-value.

This in-depth investigation aids in the assessment of the reliability and potential applications of observed station data and gridded precipitation datasets in meteorological studies by facilitating an understanding of their linkages. APHRODITE has the highest correlation (0.8) with observed station data among the gridded precipitation datasets, showing a significant positive association. Notably, the observed station data displays a strong positive correlation ($Z = 0.82$) with APHRODITE, highlighting its reliability in detecting precipitation patterns more accurately than IMDAA, CHIRPS, and CRU. The Z values, which reflect standard scores, provide an empirical measure of the significance of the correlation. APHRODITE has the highest Z value among the datasets, indicating that it is the dataset that best correlates with the observed station data. This shows that, when compared to IMDAA, CHIRPS, and CRU, APHRODITE captures the spatial precipitation patterns more accurately.

While the correlations between IMDAA and CHIRPS are minor, and CRU has a very weak positive connection, the intensity of the association with APHRODITE emphasises its accuracy in representing observed precipitation patterns. When looking for accurate gridded precipitation data that corresponds well with ground-based observations, researchers and meteorologists may find APHRODITE particularly useful, increasing their trust in its applicability for many applications in climate and hydrological studies. Table S3 displays the p-values for the relationships between observed Tmax station data and two gridded precipitation datasets, IMDAA and CRU. Both CRU and IMDAA have negative P-values, indicating statistically significant negative correlations with the observed Tmax data. However, CRU (-0.57) has a greater negative correlation and a lower P-value than IMDAA (-0.49), implying a closer alignment with the observed data. This suggests that CRU may be a more reliable alternative for locations with limited or no observed T*max* data, potentially making it helpful in data-scarce regions where accurate temperature information is critical for numerous applications in climate and environmental studies.

6. Conclusion

Understanding climate change at a regional level, such as the Jhelum basin in the Himalayas, is critical for developing effective strategies for adaptation and mitigation.

In this study, we analysed climatic variability in the Jhelum basin using meteorological parameters from different gridded datasets and observed climate data from the Indian Meteorological Department. The study is the first of its kind to perform a comparative analysis between various gridded climate data products across the Jhelum basin. It also compared gridded datasets with respective observed station data to determine the degree of bias present in various datasets, identify the best available gridded data product, and assess its feasibility for data-scarce areas in the North-Western Himalayas. It was identified that most of the gridded data products depicted unrealistic precipitation scenarios and represented increasing trends, while the actual observed precipitation depicted decreasing trends. In terms of temperature, all gridded datasets presented increasing trends but with significant differences in terms of absolute observed temperature. The IMDAA proved to be the best-gridded data product, depicting realistic trends that matched observed data but overrepresenting precipitation and showing considerable differences in areas located at higher elevations. The study emphasises the need for caution when using gridded datasets solely for precipitation assessments in complex terrains like the Himalayas. It suggests bias-correcting gridded data with observed data and refining precipitation modelling by incorporating elevation factors, resultant precipitation, and temperature variations to better understand climatic variability. This will enable the application and integration of gridded products and observed datasets in scarce and eco-sensitive areas like the Jhelum basin in the Himalayas.

Acknowledgement

The authors express sincere gratitude to the Indian Meteorological Department (IMD), Srinagar, for providing the observed datasets crucial for this study. The availability of this valuable data significantly contributed to the depth and quality of our research. We also acknowledge the following agencies for their invaluable contributions to climate science by freely providing datasets: the Asia-Pacific Water Forum's Integrated Climate Data Center (APHRODITE), the Climatic Research Unit (CRU), the Indian Meteorological Department Archive Access (IMDAA), and the Climate Hazard Group InfraRed Precipitation with Station data (CHIRPS). Their commitment to open data has been instrumental in advancing our understanding of climate dynamics.

Ethical approval

All the ethical standards of research publishing were taken care of during this study.

Disclosure statement

No potential conflict of interest was reported by the authors.

Funding

RA and IHM acknowledge the support from the BRAINSTORM project, which is a University of Leeds International Strategy Fund award.

Data availability statement

The data supporting the findings of this study are available upon reasonable request. Researchers interested in accessing the dataset and associated materials, including Python codes used in the analysis, are invited to contact the corresponding author. We are committed to promoting transparency and facilitating the reproducibility of our research.

References

Ahmad ST, Ahmed R, Wani GF, Sharma P, Ahmed P. 2022. Glacier changes in Sind basin (1990–2018) of North-western Himalayas using earth observation data. Model Earth Syst Environ. 8(2):2567–2579. 10.1007/s40808-021-01246-w.

Ahmad, S. T., Ahmed, R., Wani, G. F., Sharma, P., Ahmed, P., Mir, R. A., & Alam, J. B. (2022). Assessing the status of glaciers in upper Jhelum Basin of Kashmir Himalayas using multi-temporal satellite data. Earth Systems and Environment, 6(2), 375-389. 10.1007/s41748-021-00273-y

Ahmed R, Wani G F, Ahmad S T, Sahana M, Singh H, Ahmed P. 2021. A review of glacial lake expansion and associated glacial lake outburst floods in the Himalayan region. Earth Systems and Environment. 5(3):695–708. 10.1007/s41748-021-00230-9.

Ahmed R, Ahmad ST, Wani GF, Mir RA, Almazroui M, Bansal JK, Ahmed P. 2022. Glacial lake changes and the identification of potentially dangerous glacial lakes (PDGLs) under warming climate in the Dibang River Basin, Eastern Himalaya, India. Geocarto International. 37(27):17659–17685. 10.1080/10106049.2022.2134461.

Ahmed R, Rawat M, Wani GF, Ahmad ST, Ahmed P, Jain SK, Meraj G, Mir RA, Rather AF, Farooq M. 2022. Glacial Lake Outburst Flood Hazard and Risk Assessment of Gangabal Lake in the Upper Jhelum Basin of Kashmir Himalaya Using Geospatial Technology and Hydrodynamic Modeling. Remote Sensing. 14(23):5957 10.3390/rs14235957.

Ahmed R, Ahmad ST, Wani GF, Ahmed P, Mir AA, Singh A. 2022. Analysis of landuse and landcover changes in Kashmir valley, India—A review. GeoJournal. 87(5):4391–4403. 10.1007/s10708-021-10465-8.

Ahmed, R., Ahmad, S. T., Wani, G. F., Ahmed, P., Mir, A. A., & Singh, A. (2022b). Analysis of landuse and landcover changes in Kashmir valley, India—a review. GeoJournal, 87(5), 4391-4403. 10.1007/s10708-021-10465-8

Ahmed R, Ahmad ST, Wani GF, Mir RA, Almazroui M, Bansal JK, Ahmed P. 2022a. Glacial lake changes and the identification of potentially dangerous glacial lakes (PDGLs) under warming climate in the Dibang River Basin, Eastern Himalaya, India. Geocarto Int. 37(27): 17659–17685. doi: 10.1080/10106049.2022.2134461.

Ahsan S, Bhat MS, Alam A, Farooq H, Shiekh HA. 2022. Evaluating the impact of climate change on extreme temperature and precipitation events over the Kashmir Himalaya. Clim Dyn. 58(5–6):1651–1669. doi: 10.1007/s00382-021-05984-6.

Almazroui M. 2020. Changes in temperature trends and extremes over Saudi Arabia for the period 1978–2019. Adv Meteorol. 2020:1–21. doi: 10.1155/2020/8828421.

Andermann C, Bonnet S, Gloaguen R. 2011. Evaluation of precipitation data sets along the Himalayan front Geochem. Geochem Geophys Geosyst. 12(7). doi: 10.1029/2011GC003513.

Archer D, R &, Fowler H, J. 2004. Spatial and temporal variations in precipitation in the Upper Indus Basin, global teleconnections and hydrological implications. Hydrol Earth Syst Sci. 8(1):47–61. 10.5194/hess-8-47-2004.

Ashrit R, Indira Rani S, Kumar S, Karunasagar S, Arulalan T, Francis T, … Rajagopal E. 2020. IMDAA regional reanalysis: performance evaluation during Indian summer monsoon season. J Geophys Res. Atmos. 125(2):e2019.

Bhutiyani MR, Kale VS, Pawar NJ. 2007. Long-term trends in maximum, minimum and mean annual air temperatures across the Northwestern Himalaya during the 20th century. Clim Chang. 85(1–2):159–177. doi: 10.1007/s10584-006-9196-1.

Bhutiyani MR, Kale VS, Pawar NJ. 2010. Climate change and the precipitation variations in the northwestern Himalaya: 1866–2006. Intl J Climatol. 30(4):535–548. doi: 10.1002/joc.1920.
Bloomfield P. 1992. Trends in global temperature. Clim Change. 21(1):1–16. doi: 10.1007/BF00143250.
Buri ES, Keesara VR, Loukika KN. 2022. Long-term trend analysis of observed gridded precipitation and temperature data over Munneru River basin, India. J Earth Syst Sci. 131(2):1–18. doi: 10.1007/s12040-022-01864-7.
Caloiero T, Coscarelli R, Pellicone G. 2021. Trend analysis of rainfall using gridded data over a region of Southern Italy. Water. 13(16):2271. doi: 10.3390/w13162271.
Chambers J M, Hastie T J. 2017. Statistical models. In Statistical models. S-Routledge. :13–44.
Chatterjee S, Rangarajan S. 2022. Study and analysis of precipitation trends and variability for Karnataka State in India. In India II: climate change impacts, mitigation and adaptation in developing countries. Cham: Springer International Publishing; p. 323–349.
Dad JM, Muslim M, Rashid I, Rashid I, Reshi ZA. 2021. Time series analysis of climate variability and trends in Kashmir Himalaya. Ecol Indic. 126:107690. doi: 10.1016/j.ecolind.2021.107690.
Dahri ZH, Ludwig F, Moors E, Ahmad B, Khan A, Kabat P. 2016. An appraisal of precipitation distribution in the high-altitude catchments of the Indus basin. Sci Total Environ. 548-549:289–306. doi: 10.1016/j.scitotenv.2016.01.001.
Das M, Das A, Momin S, Pandey R. 2020. Mapping the effect of climate change on community livelihood vulnerability in the riparian region of Gangatic Plain, India. Ecol Indic. 119: 106815. doi: 10.1016/j.ecolind.2020.106815.
Dash SK, Jenamani RK, Kalsi SR, Panda SK. 2007. Some evidence of climate change in twentieth-century India. Clim Change. 85(3–4):299–321. doi: 10.1007/s10584-007-9305-9.
Das J, Treesa A, Umamahesh NV. 2018. Modelling impacts of climate change on a river basin: analysis of uncertainty using REA & possibilistic approach. Water Resour Manage. 32(15): 4833–4852. doi: 10.1007/s11269-018-2046-x.
Duhan D, Pandey A. 2013. Statistical analysis of long term spatial and temporal trends of precipitation during 1901– 2002 at Madhya Pradesh, India. Atmos Res. 122:136–149. doi: 10.1016/j.atmosres.2012.10.010.
Folland CK, Rayner NA, Brown SJ, Smith TM, Shen SSP, Parker DE, Macadam I, Jones PD, Jones RN, Nicholls N, et al. 2001. Global temperature change and its uncertainties since 1861. Geophys Res Lett. 28(13):2621–2624. doi: 10.1029/2001GL012877.
Fowler H J, Archer D R. 2006. Conflicting signals of climatic change in the Upper Indus Basin. Journal of Climate. 19(17):4276–4293. 10.1175/JCLI3860.1.
Funk C, Peterson P, Landsfeld M, Pedreros D, Verdin J, Shukla S, Husak G, Rowland J, Harrison L, Hoell A, et al. 2015. The climate hazards infrared precipitation with stations—a new environmental record for monitoring extremes. Sci Data. 2(1):150066. (doi: 10.1038/sdata.2015.66.
Gong Z, Zhao S, Gu J. 2017. Correlation analysis between vegetation coverage and climate drought conditions in North China during 2001–2013. J Geogr Sci. 27(2):143–160. 10.1007/s11442-017-1369-5.
Grotjahn R, Huynh J. 2018. Contiguous US summer maximum temperature and heat stress trends in CRU and NOAA Climate Division data plus comparisons to reanalyses. Sci Rep. 8(1):11146. doi: 10.1038/s41598-018-29286-w.
Guan L. 2009. Preparation of future weather data to study the impact of climate change on buildings. Build Environ. 44(4):793–800. doi: 10.1016/j.buildenv.2008.05.021.
Gulizia C, Camilloni I. 2016. A spatio-temporal comparative study of the representation of precipitation over South America derived by three gridded data sets. Intl J Climatol. 36(3): 1549–1559. doi: 10.1002/joc.4416.
Haile GG, Tang Q, Hosseini-Moghari S, Liu X, Gebremicael TG, Leng G, Kebede A, Xu X, Yun X. 2020. Projected impacts of climate change on drought patterns over East Africa. Earth's Future. 8(7):e2020EF001502. doi: 10.1029/2020EF001502.

Hamada A, Arakawa O, Yatagai A. 2012. An automated quality control method for daily rain-gauge data. Global Environ. 15:165–172.

Harris I, Osborn TJ, Jones P, Lister D. 2020. Version 4 of the CRU TS monthly high-resolution gridded multivariate climate dataset. Sci Data. 7(1):109. doi: 10.1038/s41597-020-0453-3.

Hosseini-Moghari SM, Araghinejad S, Ebrahimi K. 2018. Spatio-temporal evaluation of global gridded precipitation datasets across Iran. Hydrol Sci J. 63(11):1669–1688. doi: 10.1080/02626667.2018.1524986.

Hussain S, Song X, Ren G, Hussain I, Han D, Zaman MH. 2017. Evaluation of gridded precipitation data in the Hindu Kush–Karakoram–Himalaya mountainous area. Hydrol Sci J. 62(14):2393–2405. doi: 10.1080/02626667.2017.1384548.

Imbach P, Chou SC, Lyra A, Rodrigues D, Rodriguez D, Latinovic D, Siqueira G, Silva A, Garofolo L, Georgiou S. 2018. Future climate change scenarios in Central America at high spatial resolution. PLoS One. 13(4):e0193570. doi: 10.1371/journal.pone.0193570.

Imdad K, Rihan M, Sahana M, Parween S, Ahmed R, Costache R, Chaudhary A, Tripathi R. 2023. Wetland health, water quality, and resident perceptions of declining ecosystem services: a case study of Mount Abu, Rajasthan, India. Environ Sci Pollut Res Int. 30(55):116617–116643. 10.1007/s11356-022-21902-7. 35854070

Immerzeel WW, Wanders N, Lutz AF, Shea JM, Bierkens MF. 2015. Reconciling high-altitude precipitation in the upper Indus basin with glacier mass balances and runoff. Hydrol Earth Syst Sci. 19(11):4673–4687. doi: 10.5194/hess-19-4673-2015.

IPCC Core Writing Team. 2023. Summary for policymakers. In: Lee H, Romero J, editors. Climate change 2023: synthesis report. Contribution of working groups I, II and III to the Sixth Assessment Report of the intergovernmental panel on climate change. Geneva, Switzerland: IPCC; p. 1–34. doi: 10.59327/IPCC/AR6-9789291691647.001.

Ji X, Li Y, Luo X, He D, Guo R, Wang J, Bai Y, Yue C, Liu C. 2020. Evaluation of bias correction methods for APHRODITE data to improve hydrologic simulation in a large Himalayan basin. Atmos Res. 242:104964. doi: 10.1016/j.atmosres.2020.104964.

Kamiguchi K, Arakawa O, Kitoh A, Yatagai A, Hamada A, Yasutomi N. 2010. Development of APHRO_JP, the first Japanese high-resolution daily precipitation product for more than 100 years. Hydrol Res Lett. 4:60–64. doi: 10.3178/hrl.4.60.

Kumar P, Wiltshire A, Mathison C, Asharaf S, Ahrens B, Lucas-Picher P, Christensen JH, Gobiet A, Saeed F, Hagemann S, et al. 2013. Downscaled climate change projections with uncertainty assessment over India using a high resolution multi-model approach. Sci Total Environ. 468–469 Suppl:S18–S30. doi: 10.1016/j.scitotenv.2013.01.051.

Lee H, Calvin K, Dasgupta D, Krinner G, Mukherji A, Thorne P, … Zommers Z. 2023. AR6 Synthesis report: climate change 2023. In: Summary for policymakers.

Lone BA, Qayoom S, Nazir A, Ahanger SA, Basu U, Bhat TA, Dar ZA, Mushtaq M, Sabagh AE, Soufan W, et al. 2022. Climatic trends of variable temperate environment: a complete time series analysis during 1980–2020. Atmosphere. 13(5):749. doi: 10.3390/atmos13050749.

Mahmood S, Davie J, Jermey P, Renshaw R, George JP, Rajagopal EN, Rani SI. 2018. Indian monsoon data assimilation and analysis regional reanalysis: configuration and performance. Atmos Sci Lett. 19(3):e808. doi: 10.1002/asl.808.

Malik IH. 2022a. Spatial dimension of impact, relief, and rescue of the 2014 flood in Kashmir Valley. Nat Hazards (Dordr). 110(3):1911–1929. doi: 10.1007/s11069-021-05018-8.

Malik IH. 2022b. Anthropogenic causes of recent floods in Kashmir Valley: a study of 2014 flood. SN Soc Sci. 2(8):162. doi: 10.1007/s43545-022-00463-z.

Malik IH, Ford JD. 2024a. Monitoring climate change vulnerability in the Himalayas. Ambio: 1–19. doi: 10.1007/s13280-024-02066-9.

Malik IH, Ford JD. 2024b. Addressing the climate change adaptation gap: key themes and future directions. Climate. 12(2):24. doi: 10.3390/cli12020024.

Marazi, AA. 2019. Modelling the Contribution of Glacier melt Snow melt Rainfall and Baseflow to Lidder River, 2019

Malik IH, Hashmi SNI. 2021. The great flood and its aftermath in Kashmir Valley: impact, consequences and vulnerability assessment. J Geol Soc India. 97(6):661–669. doi: 10.1007/s12594-021-1742-y.

Malik IH, Hashmi SNI. 2022. Ethnographic account of flooding in North-Western Himalayas: a study of Kashmir Valley. GeoJournal. 87(2):1265–1283. doi: 10.1007/s10708-020-10304-2.

Malik IH, Ahmed R, Ford JD, Shakoor MSA, Wani SN. 2024. Beyond the banks and deluge: understanding riverscape, flood vulnerability, and responses in Kashmir. Natural Hazards. :1–22.

Mir RA, Ahmed R, Hussain M, Bukhari SK, Ahmed P, Dar R, … & Bhat W. (2024). Causes, concernsofsinkholeformationinBrengistreamcatchmentofUpperJhelumbasin,KashmirHimalaya. Environ Dev Sustain. 26(6): 14507–14534. doi: 10.1007/s10668-023-03204-1.

Mondal A, Kundu S, Mukhopadhyay A. 2012. Rainfall trend analysis by Mann-Kendall test: a case study of North-Eastern part of Cuttack district. Orissa. Int J Geol Earth and Environ Sci. 2(1):70–78. ISSN:227–2081.

Mutti PR, Dubreuil V, Bezerra BG, Arvor D, de Oliveira CP, Santos e Silva CM. 2020. Assessment of gridded CRU TS data for long-term climatic water balance monitoring over the Sao Francisco Watershed, Brazil. Atmosphere. 11(11):1207. doi: 10.3390/atmos11111207.

Nourani V, Danandeh Mehr A, Azad N. 2018. Trend analysis of hydroclimatological variables in Urmia Lake basin using hybrid wavelet Mann–Kendall and Şen tests. Environ Earth Sci. 77(5):1–18. doi: 10.1007/s12665-018-7390-x.

Pai DS, Sridhar L, Rajeevan M, Sreejith OP, Satbhai NS, Mukhopadhyay B. 2014. Development of a new high spatial resolution (0.25° X 0.25°) Long period (1901-2010) daily gridded rainfall data set over India and its comparison with existing data sets over the region. MAUSAM. 65(1):1–18. january 2014doi: 10.54302/mausam.v65i1.851.

Pal AB, Khare D, Mishra PK, Singh L. 2017. Trend analysis of rainfall, temperature and runoff data: a case study of Rangoon watershed in Nepal. ijsrtm. 5(3):21–38. doi: 10.18510/ijsrtm.2017.535.

Palazzi E, Hardenberg JV, Provenzale A. 2013. Precipitation in the HinduKush Karakoram Himalaya: observations and future scenarios. J. Geophys. Res. Atmos. 118(1):85–100.

Paredes-Trejo FJ, Barbosa HA, Kumar TL. 2017. Validating CHIRPS-based satellite precipitation estimates in Northeast Brazil. J Arid Environ. 139:26–40. doi: 10.1016/j.jaridenv.2016.12.009.

Patel P, Thakur PK, Aggarwal SP, Garg V, Dhote PR, Nikam BR, Swain S, Al-Ansari N. 2022. Revisiting 2013 Uttarakhand flash floods through hydrological evaluation of precipitation data sources and morphometric prioritization. Geomatics, Nat Hazards and Risk. 13(1):646–666. doi: 10.1080/19475705.2022.2038696.

Radhakrishnan K, Sivaraman I, Jena SK, Sarkar S, Adhikari S. 2017. A climate trend analysis of temperature and rainfall in India. Clim Chang and Environ Sustain. 5(2):146–153. doi: 10.5958/2320-642X.2017.00014.X.

Rani SI, T A, George JP, Rajagopal EN, Renshaw R, Maycock A, Barker DM, Rajeevan M. 2021. IMDAA: high-resolution satellite-era reanalysis for the Indian monsoon region. J Climate. 34(12):1–78. doi: 10.1175/JCLI-D-20-0412.1.

Rao Y, Liang S, Yu Y. 2018. Land surface air temperature data are considerably different among BEST-LAND, CRU-TEM4v, NASA-GISS, and NOAA-NCEI. JGR Atmospheres. 123(11):5881–5900. doi: 10.1029/2018JD028355.

Rather, A. F., Ahmed, R., Ahmed, P., Bansal, J. K., Banerjee, P., Wani, T. A.,..&Mir, R. A. (2024). Examining the glacier-glacial lake interactions of potentially dangerous glacial lakes (PDGLs) under changing climate in Shyok catchment of the Upper Indus Basin. Physics and Chemistry of the Earth, Parts A/B/C, 136, 103686. 10.1016/j.pce.2024.103686

Rawat M, Jain SK, Ahmed R, Lohani AK. 2023. Glacial lake outburst flood risk assessment using remote sensing and hydrodynamic modeling: a case study of Satluj basin, Western Himalayas, India. Environ Sci Pollut Res Int. 30(14):41591–41608. 10.1007/s11356-023-25134-1. 36633748

Reda KW, Liu X, Tang Q, Gebremicael TG. 2021. Evaluation of global gridded precipitation and temperature datasets against gauged observations over the Upper Tekeze River Basin, Ethiopia. J Meteorol Res. 35(4):673–689. doi: 10.1007/s13351-021-0199-7.

Romshoo SA, Bashir J, Rashid I. 2020. Twenty-first century-end climate scenario of Jammu and Kashmir Himalaya, India, using ensemble climate models. Clim Change. 162(3):1473–1491. doi: 10.1007/s10584-020-02787-2.

Sabin TP, Krishnan R, Vellore R, Priya P, Borgaonkar HP, Singh BB, Sagar A. 2020. Climate change over the Himalayas. In: Assessment of climate change over the Indian region. Singapore: Springer; p. 207–222.

Shafiq M U, Rasool R, Ahmed P, Dimri A P. 2019. Temperature and precipitation trends in Kashmir Valley, north western Himalayas. Theoretical and Applied Climatology. 135:293–304. 10.1007/s00704-018-2377-9.

Sharmila S, Joseph S, Sahai AK, Abhilash S, Chattopadhyay R. 2015. Future projection of Indian summer monsoon variability under climate change scenario: An assessment from CMIP5 climate models. Global Planet Change. 124:62–78. doi: 10.1016/j.gloplacha.2014.11.004.

Shrestha AB, Wake CP, Mayewski PA, Dibb JE. 1999. Maximum temperature trends in the Himalaya and its vicinity: an analysis based on temperature records from Nepal for the period 1971–94. J Climate. 12(9):2775–2786. doi: 10.1175/1520-0442(1999)012<2775:MTTITH>2.0.CO;2.

Shrestha AB. 2009. Climate change in the Himalayas. Kathmandu. International Centre for Integrated Mountain Development and United Nations Environment Programme Regional Office, Asia and the Pacific. (ICIMOD Publication 3/09.).

Sidau, M. R., Horváth, C., & Cheveresan, M. (2021).,andric,I.;,F.AssessingHydrologicalImpactof ForestedAreaChange:RemoteSensingCaseStudy.Atmosphere,12,817. 10.3390/atmos12070817

Singh BK, Bardgett RD, Smith P, Reay DS. 2010. Microorganisms and climate change: terrestrial feedbacks and mitigation options. Nat Rev Microbiol. 8(11):779–790. doi: 10.1038/nrmicro2439.

Singh V, Xiaosheng Q. 2019. Data assimilation for constructing long-term gridded daily rainfall time series over Southeast Asia. Clim Dyn. 53(5–6):3289–3313. doi: 10.1007/s00382-019-04703-6.

Steger S, Mair V, Kofler C, Pittore M, Zebisch M, Schneiderbauer S. 2021. Correlation does not imply geomorphic causation in data-driven landslide susceptibility modelling- Benefits of exploring landslide data collection effects. Sci Total Environ. 776:145935 10.1016/j.scitotenv.2021.145935. PMC: 33652311

Sulugodu B, Deka PC. 2019. Evaluating the performance of CHIRPS satellite rainfall data for streamflow forecasting. Water Resour Manage. 33(11):3913–3927. doi: 10.1007/s11269-019-02340-6.

Swain S, Mishra SK, Pandey A. 2022b. Assessing spatiotemporal variation in drought characteristics and their dependence on timescales over Vidarbha Region, India. Geocarto Int. 37(27):17971–17993. doi: 10.1080/10106049.2022.2136260.

Swain S, Mishra SK, Pandey A, Dayal D. 2022a. Spatiotemporal assessment of precipitation variability, seasonality, and extreme characteristics over a Himalayan catchment. Theor Appl Climatol. 147(1–2):817–833. doi: 10.1007/s00704-021-03861-0.

Swain S, Mishra SK, Pandey A, Dayal D, Srivastava PK. 2022c. Appraisal of historical trends in maximum and minimum temperature using multiple non-parametric techniques over the agriculture-dominated Narmada Basin, India. Environ Monit Assess. 194(12):893. doi: 10.1007/s10661-022-10534-6.

Swain S, Mishra SK, Pandey A, Pandey AC, Jain A, Chauhan SK, Badoni AK. 2022d. Hydrological modelling through SWAT over a Himalayan catchment using high-resolution geospatial inputs. Environ Challenges. 8:100579. doi: 10.1016/j.envc.2022.100579.

Wagner P D, Fiener P, Wilken F, Kumar S, Schneider K. 2012. Comparison and evaluation of spatial interpolation schemes for daily rainfall in data scarce regions. Journal of Hydrology. :388–400. 46410.1016/j.jhydrol.2012.07.026.

Wani GF, Ahmed R, Ahmad ST, Singh A, Walia A, Ahmed P, Shah AA, Mir RA. 2022. Local perspectives and motivations of people living in flood-prone areas of Srinagar city, India. Int J Disaster Risk Reduct. 82:103354. doi: 10.1016/j.ijdrr.2022.103354.

Xu J, Grumbine RE, Shrestha A, Eriksson M, Yang X, Wang YUN, Wilkes A. 2009. The melting Himalayas: cascading effects of climate change on water, biodiversity, and livelihoods. Conserv Biol. 23(3):520–530. doi: 10.1111/j.1523-1739.2009.01237.x.

Yadav R, Tripathi SK, Pranuthi G, Dubey SK. 2014. Trend analysis by Mann-Kendall test for precipitation and temperature for thirteen districts of Uttarakhand. J Agrometeorol. 16(2): 164–171.

Yan M, Xue M, Zhang L, Tian X, Chen B, Dong Y. 2021. A decade's change in vegetation productivity and its response to climate change over Northeast China. Plants. 10(5):821 10.3390/plants10050821.

Yasutomi N, Hamada A, Yatagai A. 2011. Development of a long-term daily gridded temperature dataset and its application to rain/snow discrimination of daily precipitation. Global Environ Res:V15N2.

Yatagai A, Kamiguchi K, Arakawa O, Hamada A, Yasutomi N, Kitoh A. 2012. APHRODITE: Constructing a long-term daily gridded precipitation dataset for Asia based on a dense network of rain gauges. Bulletin of the American Meteorological Society. 93(9):1401–1415. 10.1175/BAMS-D-11-00122.1.

Yin H, Donat MG, Alexander LV, Sun Y. 2015. Multi-dataset comparison of gridded observed temperature and precipitation extremes over China. Intl J Climatol. 35(10):2809–2827. doi: 10.1002/joc.4174.

Yu D, Liu Y, Shi P, Wu J. 2019. Projecting impacts of climate change on global terrestrial ecoregions. Ecol Indic. 103:114–123. doi: 10.1016/j.ecolind.2019.04.006.

Zaki S A, Syahidah S W, Shahidan M F, Ahmad M I, Yakub F, Hassan M Z, Md Daud M Y. 2020. Assessment of outdoor air temperature with different shaded area within an urban university campus in hot-humid climate. Sustainability. 12(14):5741 10.3390/su12145741.

Zaz SN, Romshoo SA, Krishnamoorthy RT, Viswanadhapalli Y. 2019. Analyses of temperature and precipitation in the Indian Jammu and Kashmir region for the 1980–2016 period: implications for remote influence and extreme events. Atmos Chem Phys. 19(1):15–37. 10.5194/acp-19-15-2019.